Perspective: High pressure transformations in nanomaterials and opportunities in material design

Denis Machon, Vittoria Pischedda, Sylvie Le Floch, Alfonso San-Miguel

Journal of Applied Physics

Perspective: High pressure transformations in nanomaterials and opportunities in material design

Cite as: J. Appl. Phys. **124**, 160902 (2018); https://doi.org/10.1063/1.5045563
Submitted: 21 June 2018 . Accepted: 12 October 2018 . Published Online: 29 October 2018

Denis Machon, Vittoria Pischedda, Sylvie Le Floch, and Alfonso San-Miguel

JOURNAL OF APPLIED PHYSICS **124**, 160902 (2018)

Perspective: High pressure transformations in nanomaterials and opportunities in material design

Denis Machon, Vittoria Pischedda, Sylvie Le Floch, and Alfonso San-Miguel
CNRS, Institut Lumière Matière, Univ Lyon, Université Claude Bernard Lyon 1, F-69622 Villeurbanne, France

(Received 21 June 2018; accepted 12 October 2018; published online 29 October 2018)

Pressure and temperature phase transitions of nanomaterials often differ significantly from those of their bulk parents, offering novel approaches for the engineering of original materials. The importance or even the dominance of surface atoms in the nanoworld enhances the effects of environment, geometry, and intercalation. In the present article, we explore the current knowledge of these effects, as evidenced in the high pressure phase diagrams of nanomaterials such as nanocrystals, carbon nanotubes, fullerites, graphene, and other 2D systems, as well as nanoporous structures like clathrates or zeolites. Recent advances and future challenges in the use of extreme thermodynamic conditions to develop new functional nanomaterials, composites, or devices will be reviewed, along with the specificities of the experimental environment required for these investigations. *Published by AIP Publishing.* https://doi.org/10.1063/1.5045563

I. INTRODUCTION

Moving from the macroscale to the nanoscale may lead to severe changes in the physical and chemical properties of materials. Quantum confinement effects and/or the increasing prevalence of surface atoms drives physical evolutions between bulk and nanoscaled materials. Nanoscale can also bring topological changes, which can induce drastic modifications in physical properties. As such, nanotube shaped objects, nanospheres, and bidimensional sheets of the same bonded atoms can exhibit totally different behaviors. How are the high pressure properties of nano-objects and nanomaterials influenced by nanosize and topology? What opportunities are there for the design of new materials?

The aim of this perspective is many-fold. First, we want to provide a panorama on the various high pressure transformations (sometimes combined with high temperature conditions) in different classes of nanosystems and nanomaterials. We will emphasize, in parallel, those aspects of the nanoworld that clearly make a difference with respect to bulk materials and that may determine the particular phase diagram of the system: size or geometry effects, the interaction with the environment, and intercalation. These aspects are of great interest and require a timely perspective in order to provide the reader with different elements allowing engineering new nanomaterials through severe quasi-hydrostatic mechanical compressive methods. Without pretending to offer a complete review of high pressure nanophysics, we aim to focus on those aspects which appear to us as crucial for future research on the design of new materials. They will be summarized in Sec. VI.

Under high pressure in the GPa or tenths of GPa regime, the atomic volume of bulk materials can be reduced by 10% or more. The associated bond length contraction leads to important changes in the material properties, including the electronic structure. With progressive compression, some atomic organizations may be favored and phase transitions between different crystallographic structures may take place.[1] The majority of such phase transitions are of first-order in the thermodynamic sense, and the associated kinetics plays a central role. Below the spinodal limit (on compression or decompression), metastable phases can be preserved (diamond at ambient conditions, for instance) allowing for the convergence of condensed matter physics and material engineering. Transformations in the metastable regime may also lead to the appearance of amorphous states.[2]

At nanoscale, the prominence of surface atoms, with their different contribution to the cohesive energy through their associated surface energy, can totally modify a phase energy landscape with many different consequences.[3] Depending on the importance of such modifications, the phase diagram of a nanomaterial relative to its bulk parent may (i) just shift with changes in the transition pressures; (ii) involve new crystallographic structures; (iii) amorphous states; or (iv) even introduce the (meta)stabilization of new phases. Nanosize allows the fine-tuning of the phase diagram by changing the ratio of surface and bulk atoms. In addition, shapes of nanoclusters or nanoparticles (spheres, tubes, polygons, etc.), i.e., geometry and topology, can also offer novel opportunities for phase diagram modifications.

The increased proportion of atoms at the surface of a nanoparticle allows for many different interactions with its environment. It can be a way of modifying the surface energy through adsorption and the surface chemistry, leading to modified phase diagrams of nanomaterials. In open nanosystems, i.e., those with cavities of different shapes, intercalation/insertion of molecules or ions is possible, with the potential for continuous tuning of electronic properties which can be enhanced or modified through the application of pressure. Further modifications of such hosted molecules or ions with the use of pressure may be another parameter for tuning the material properties. Many high pressure experiments are performed using a fluid pressure transmitting medium (PTM). Depending on its physico-chemical characteristics, the PTM can participate in the phase diagram definition of

the nanosystem through its surface interaction or even due to its incorporation in the nanoscale system.

Another category of modifications is related to the assembling opportunities provided by the discrete nature of nano-objects. The most direct assembling strategy may just involve the nano-constituents themselves, linked through new bonds. This is, for instance, the case for fullerenes with 1D, 2D, and 3D polymers obtained through treatment at extreme conditions of pressure and temperature. Other examples include the case of carbon nanotubes or clathrate phases. Pressure-enhanced interactions between the nano-objects and their environment may lead to the synthesis of nanocomposites that are already used in many different applications. This category of materials is enjoying rapid growth and development.[4]

Finally, nanostructuration allows the introduction of additional interfaces which can have a dramatic effect on the mechanical properties of materials, as underlined by the Hall-Petch law and the inverse Hall-Petch variants at the nanoscale. The high pressure synthesis of nano-polycrystalline diamond,[5] with hardness surpassing that of single-crystalline diamond, constitutes the outstanding example of the opportunities offered by nanostructuration on the design of new materials.

The manuscript is organized in 7 sections. In Sec. II, we will discuss the specific methods for generating high pressure and high temperature (HP-HT) conditions. We will concentrate on recent advances which have been specifically developed to cope with the challenges associated to the study of nanomaterials. Secs. III–V will cover our knowledge on the opportunities for material design considering: nano-objects size and geometry (Sec. III), the effects of the interaction with the environment (Sec. IV), and the consequences of intercalation/insertion of atomic or molecular species (Sec. V). We will finally discuss, in Sec. VI, a number of applications arising from the high pressure processing of nanomaterials and explore some future perspectives offered by nanomaterials submitted to high pressures in the development of new materials.

II. HIGH PRESSURE AND HIGH TEMPERATURE GENERATION

The main techniques used to investigate nanomaterials at HP-HT are diamond anvil cells (DACs) and large volume presses (LVPs). Both techniques combine pressure and temperature in a static way to explore the matter transformations and associated chemical and physical property changes in a vast P-T space. Dynamic pressure methods are sometimes also employed, including detonation which has found applications for instance in nanodiamond synthesis.[6] However, we will focus on static methods which are more extensively used.

In DACs, the sample, immersed in a compressible fluid —the pressure transmitting medium, is placed in a compression chamber, formed by a pierced metal gasket, and squeezed between the polished culets of two opposed diamonds. Pressures from 1 to 400 GPa[7] or more—can be generated using diamonds with culet diameters from 1 mm to 20 μm, giving sample volumes from several thousands to few μm^3. The fluid PTM is chosen according to the desired temperature and pressure and the potential chemical or physical interaction with the sample. Methanol-ethanol mixture, silicone oil, and inert gases such as argon, neon, or helium are commonly used. Hydrostatic pressure conditions can be maintained as far as the PTM is gas or a liquid, but under sufficiently high pressure all PTM will transform into a solid. Soft van der Waals type solids can also be used as PTM. In such cases, we will speak about "quasi-hydrostatic conditions." The limits of hydrostaticity and quasi-hydrostaticity of different PTMs have been extensively reviewed in Ref. 8. The dominance of surface atoms in nanosystems and nanomaterials makes interaction with the PTM a major issue in high pressure experiments. If chemical inertness cannot be guaranteed, a modification of the system and an influence of the PTM on the phase diagram can then be expected. Some nanosystems such as nanotubes may in certain conditions allow for the insertion of the atoms or molecules of the PTM in the constitutive volume, and this can strongly influence their high pressure evolution. Those specific aspects will be discussed in Secs. IV and V when appropriate.

The working temperature range of DACs extends from 4 K to more than 3000 K. The entire DAC can be cooled down to 4 K in a cryostat or heated up to 700 K by a band heater. A small resistive oven placed inside the cell around the diamonds allows to reach 1200 K.[9] In this case, the DAC needs to be enclosed in vacuum or in an inert atmosphere to avoid deterioration of the diamond anvils and oxidation of the heater resistance. Higher temperatures are achieved by laser heating. In that case, an infrared (CO_2, Nd:YAG, Nd:YLF) laser is focused through the diamond windows on an absorbing sample or an absorber placed next to the sample.[10] The precise control over temperature is limited by the heat transfer to the sample and to the diamond anvils, and it can be challenging to measure the precise temperature obtained. Careful preparation of the cell setup is required to minimize the temperature gradient and avoid damaging the diamond anvils. Thanks to recent technical progress, the laser heating DAC is now a routine setup coupled with *in situ* X-ray diffraction or spectroscopy measurements. DAC, with its very small sample volume, is not appropriate for material synthesis but is a great tool for the *in situ* exploration of condensed matter phase behavior and properties in a wide range of pressure and temperature. As diamonds are transparent from IR to X-ray, samples can be analyzed *in situ* using X-rays (diffraction, spectroscopy, scattering, imaging, x-ray absorption spectroscopy)[7,11,12] or vibrational spectroscopy (Raman,[13] IR,[14] and photoluminescence[15]). Electrical resistivity, magnetic susceptibility, thermoelectric power, and specific heat measurements are also performed in DACs at low temperature.[16–19] DACs have been used to explore the physical properties of powders of nanocrystals, nanotubes, or nanowires. The loading of such samples in a DAC does not differ from that of their bulk analogues. Substrate-supported nano-objects such as graphene require the loading of both the nano-object and the substrate. This can be achieved using cleaved crystalline substrates some tenths of microns thick.[20,21]

LVP devices are designed for materials synthesis at HP-HT. Some devices also include characterization

possibilities such as *in situ* X-ray diffraction,[22,23] thermal analysis,[24] electrical measurements,[25,26] or acoustic velocity measurements.[27] They can be found currently integrated at many beamlines of synchrotron and neutron sources.[28] LVP may be classified into four types of pressure devices: piston cylinder ($V_{sample} < 400\,mm^3$, $P < 5$ GPa), belt apparatus ($V_{sample} = 40\,mm^3$ to $1\,dm^3$, $P < 10$ GPa),[29,30] opposed anvil systems [$V_{sample} = 1\,mm^3$ to $60\,cm^3$, $P < 12$ GPa using WC anvils[31] or up to 17 GPa with Sintered Diamond (SD) anvils[23]], and multi-anvils ($V_{sample} = 0.1\,mm^3$ to $2\,cm^3$,[32] $P < 30$ GPa with WC anvils or 100 GPa with SD anvils[33]). In all these devices, pressure is generated by the volume reduction of a compression chamber through the displacement of pistons or anvils under a force (0.1 to 300 MN) applied with a hydraulic press. Depending on the desired pressure and sample volume, the high pressure apparatus size varies from small and portable (≈50 kg)[23] to huge (several tens of tons).[30] Piston cylinder, opposed anvils, and belt apparatus are uniaxial devices where quasi-hydrostatic pressure transmitting medium (pyrophyllite, NaCl, MgO, limestone) placed as a gasket around the sample reduces the pressure gradient. The compression along several axes in the multi-anvil devices allows more hydrostatic pressure on the sample. In all these HP-HT devices, the sample is placed in a cylindrical heater (made of graphite, molybdenum, lanthanum chromite, or TiC) into a gasket which transmits the pressure and provides thermal and electrical insulation. The furnace, electrically powered through the anvils or pistons, allows to reach temperatures as high as 2000 °C.[34]

More compact cells for resistivity[35,36] or specific heat measurements[37] at low temperatures or/and high magnetic fields use inert liquid or gas as PTM to reach 7 and 1 GPa, respectively. For instance, Caillier *et al.*[36] developed a setup [Fig. 1(B)] to measure the resistivity of individual nano-objects as carbon nanotubes up to 1 GPa and low temperature.[38]

III. SIZE AND GEOMETRY EFFECTS

We first introduce here how size and geometry can modify the phase diagram with respect to the bulk and determine new physical properties. We will, in particular, discuss the case of nanocrystals and nanotubes, in which size and even geometry can be modified on almost an atom-by-atom basis. We will concentrate our discussion on the phase diagram modification as key means for engineering new materials.

A. Nanocrystals

Phase stability in finite-sized materials can be modified by surface energy control. However, if the concept of surface energy exists to describe free nanoparticle properties, this model can hardly be generalized to describe phase transitions, in particular, in high-pressure experiments. As a matter of fact, nanoparticles are embedded in a medium, a situation that creates interface energy. In general, the nature of this interface (chemical interaction, defects, etc.) may determine the phase equilibria. To better understand the effect of interface energy on phase stability, the combination of pressure and particle size is particularly important as, keeping the particle size constant, pressure allows the energy landscapes of the system to be explored, and emphasizes the contribution of interface energy in phase stability.

When dealing with nanocrystals under pressure, two main behaviors may be distinguished:

(1) If a pressure-induced phase transition occurs between a phase I and a phase II in a bulk sample, the transition pressure changes (generally increases) when decreasing the particle size.
(2) New phase and states (new polymorphs or amorphous state) compared to the bulk are observed in the (size, pressure) phase diagram.

The first case is observed in CdSe, for instance,[39] for which a $1/r$ variation of the transition pressure may be observed, where r is the particle size. This effect is understood by considering the appropriate thermodynamics potential, including the interface energy contribution, and the tendency of the high-pressure phase surface energy to be higher than that of the low-pressure phase leading to an upshift of the transition pressure.[39,40] Using the Landau theory of phase transition, a similar result is obtained by treating the difference of surface energies as a secondary order parameter.[40] However, even though several models with increasing complexity have been proposed in the literature, it is difficult to fully validate them because of experimental discrepancies.[41]

Actually, if this effect seems general, great care should be taken to define the transition pressure in nanocrystals. From most experiments, the transition pressure is defined either as the appearance of the high-pressure phase or at the disappearance of the low-pressure phase or even at the middle of the transition width. This point is crucial because a concomitant effect of pressure-induced phase transitions in nanosize systems is the broadening of the transition width (pressure range where low- and high-pressure phases coexist).

For instance, in the case of ZnO, a *1/r*-dependence of the transition pressure has been proposed[42] with r the characteristic size of the nanocrystal. However, a closer look to the experimental reports indicates that the same definition of the transition pressure has not been used (Fig. 2). Taking into account the transition width makes the interpretation more complex. No clear size-dependence (as a *1/r* law) can be drawn. Even though below 15 nm the transition occurs at a higher pressure than for the bulk, it should be noted that these nanoparticles (obtained by ball-milling, for instance) can also be more defective.

A more recent high-pressure study using the same experimental protocol was performed on ZnO nanoparticles of similar size obtained by different synthesis paths.[40] The main conclusions are that transition features (transition start and end pressures, transition width, high-pressure phases) differ in all cases and are mainly related to the presence of defects.

Therefore, as a first conclusion, it is difficult to extract a simple size-effect when aggregating several experimental studies. Some precautions are required concerning the sample characterization and an experimental protocol must be followed during high-pressure investigations of

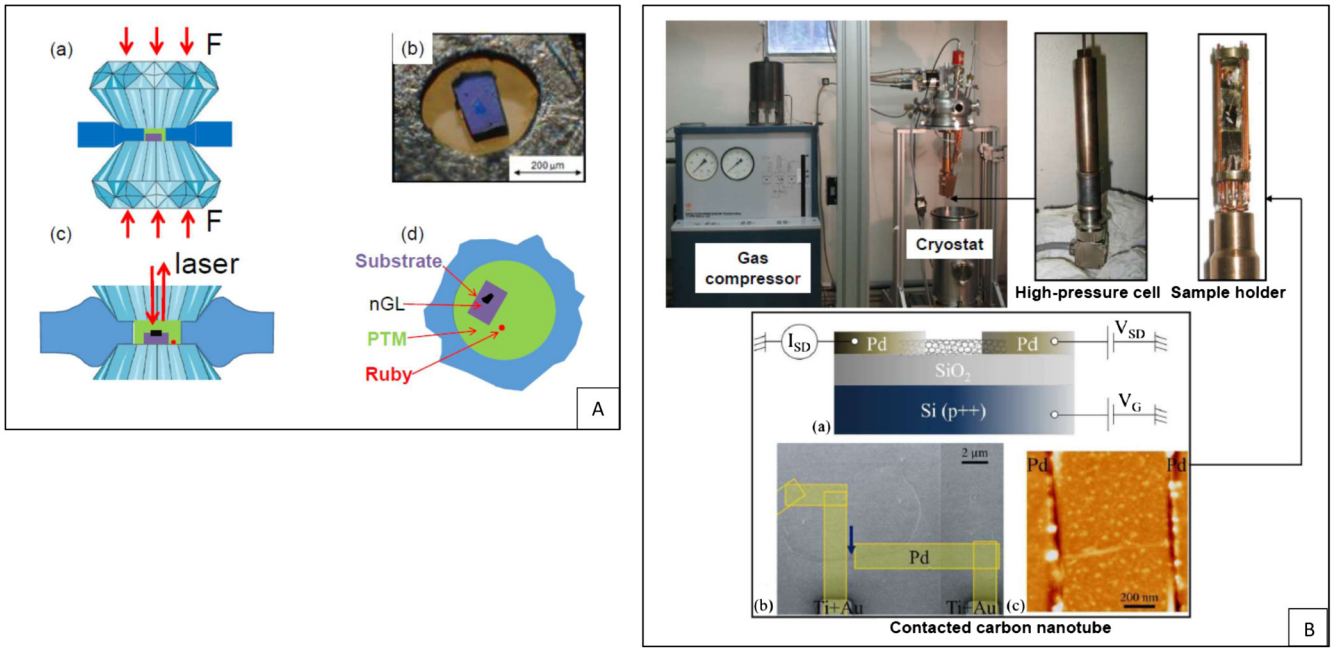

FIG. 1. (A) Supported graphene loaded in a diamond anvil cell for *in situ* high pressure Raman spectroscopy experiments.[20] (a) Schematic view of a diamond anvil cell. The gasket is squeezed between two diamonds. [(b) and (d)] Nano-graphene layer (nGL) deposed on a substrate and placed in the compression chamber. Argon is used as PTM. (c) Raman spectroscopy is performed through the diamond; (B) high pressure-low temperature transport experimental setup on a carbon nanotube (CNT) up to 1 GPa and down to 10 K.[38] Helium is used as PTM. CNT is grown by CVD on Si/SiO_2 substrate and Pd electrodes are lithographed.

nanoparticles in order to obtain a coherent, reliable set of data which can be of use by the scientific community.[40]

Secondly, such width broadening of the transition seems to be a general feature in pressure-induced phase transitions in nanoparticles. This width broadening of the transition can be interpreted in the framework of the Ginzburg-Landau theory of phase transition.[40] In that case, spatial inhomogeneities of the order parameter are treated by introducing a kinetics term using a gradient of the order parameter. It has been shown that increasing this term induces a slowing down of the transition and leads to the broadening of the transition as observed experimentally. Inhomogeneities may be due to point defects, interface, pressure gradient, etc.

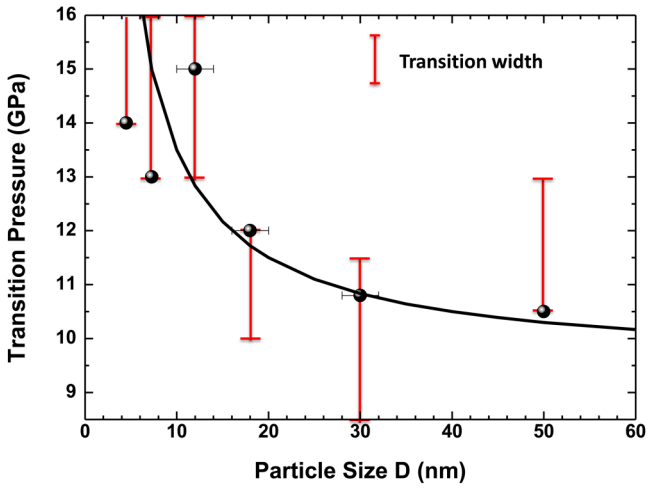

FIG. 2. Transition pressures reported in the literature (points) for ZnO nanoparticles as function of their characteristic size. An apparent $1/r$-law fits the experimental data. However, when including the transition width as error bars—defined from the appearance of the high-pressure phase to the disappearance of the low-pressure phase—a more complex picture rises (see text). Original data from Refs. 43–46.

It is interesting to note that such approach is also used to describe the amorphization process (in the case of radiation-induced amorphization[47]). In this case, increasing the kinetics term favors the amorphous state. Therefore, there is a competition between the polymorphic transition that may be slowed down by an increasing kinetics term and the amorphization process favored by the same term. It may happen that a crossing occurs, leading to a size-dependent pressure-induced amorphization.[48]

In a more sophisticated description, introducing the fractal geometry of the amorphous network, it has been shown that in nanometric systems, pressure-induced amorphization should even occur at a lower transition than the expected polymorphic transformation. This is what is observed experimentally in TiO_2, Y_2O_3, PbTe, etc.[48,49]

Some systems have different polymorphs that have a close Gibbs energy. For instance, bulk TiO_2 exhibits three polymorphs at ambient conditions: rutile, anatase, and brookite. Rutile is the stable polymorph whereas the others are metastable phases at ambient conditions. However, including an interface energy term may modify the relative Gibbs energy and stabilize a new polymorph in nanomaterials. In nano-TiO_2, the stabilized phase is the anatase structure. In consequence, the subsequent pressure-induced phase transformations are modified with appearance of new phases compared to the bulk phase diagram.[50]

The combination of the thermodynamics (interface energy contribution) and kinetics effects leads to a complex behavior of nanomaterials under high-pressure. This represents an

opportunity to gain fundamental understanding on phase transitions and metastability. In addition, pressure and particle size are two parameters that can be used conjointly to stabilize new phases that may have potential interest as functional materials. The decompression path may be also affected at the nanoscale. As kinetics effects broaden the metastability range of the different phases, this may lead to the possibility of recovering the high-pressure phase at ambient conditions.[51]

In conclusion, inhomogeneities play a significant role at the nanoscale as, with size reduction, the interfacial energy becomes comparable to the intra-particle cohesive energy. Therefore, the pressure-size phase diagram is highly dependent on the starting sample characteristics. Depending on the defects density, capping molecules (usually adsorbed molecules at the nanoparticle surface), etc., experimental observations may differ. Therefore, the pressure-size phase diagram is a projection from a more complex multi-dimensional phase diagram.[48] Figure 3 illustrates this idea taking into account a third dimension, representing inhomogeneity, in addition to pressure and size. The diagram obtained for an ideal sample ($K = 0$) may differ from a sample with point defects, for instance ($K \neq 0$).

It has to be noted that the majority of nanoparticles studied under pressure have a diameter of several nanometers which gives a system where classical thermodynamics approaches may be used. The critical particle size where these approaches cannot be invoked anymore remains to be determined and certainly depends on the system (composition, bonding, etc.).

B. Nanotubes

The tubular geometry constitutes a real topological change with respect to the fully dense nanoparticles. The new topology introduces not only geometrical constraints which may lead to totally different phase diagrams but also induce strong modifications in the environment interaction mechanisms in particular through endohedral filling.

One of the most important effects of high pressures on carbon nanotubes is the pressure-induced deformation of their cross section. Geometrically, the change of cross section implies the presence of at least four critical points due to the four vertex theorem for closed plane curves, in other words, the formation of at least two lobes (Fig. 4). This effect has been investigated in many theoretical[52–56] and experimental works.[57–64] Many studies predict an ovalization pressure followed by a collapse pressure both proportional to ϕ^{-3}, with ϕ being the tube diameter. This remarkable size effect on the pressure evolution of carbon nanotubes corresponds to the well-known behavior of macroscopic tubes, the Lévy-Carrier law.[65] Recently, it has been shown that deviations from the Lévy-Carrier law are observed for tube diameters below ~1 nm.[66] In this case, the localization of compliances due to the atomic discretization leads to a reduction of the collapse pressure which becomes zero for $\phi_m \sim 0.4$ nm, the smallest observed free standing single-walled carbon nanotube diameter. In other words, single wall carbon nanotubes (SWCNTs) deviate from a continuum mechanism description for tube diameters lower than ~1 nm. Nanotube bundling has shown to lead to a further stabilization effect with respect to the Lévy-Carrier law for tube diameters beyond 1 nm.[67] For larger diameters, the van der Waals interaction between the internal walls of the carbon nanotubes should lead to the collapse at ambient pressure at a maximum tube diameter, ϕ_M, as it has been extensively discussed in Ref. 68. The relation of collapse pressure with diameter for SWCNTs is presented in Fig. 4(e).

The collapse pressure of multi-wall carbon nanotubes (MWCNTs) has also been investigated. It has been shown in double-walled carbon nanotubes that the external tube screens the internal one from pressure effects.[70,71] The same effect is also observed in triple-wall carbon nanotubes.[72] Raman spectroscopy studies on double wall carbon nanotubes show that the pressure collapse can take place in a cascade mode with the external tube starting to deform and inducing at a higher pressure the collapse of the inner tube and then of the whole system.[13] Moreover, a recent combined experimental and theoretical work indicates that for few-wall carbon nanotubes, the Lévy-Carrier law is preserved by replacing the tube diameter, $\boldsymbol{d}$, by the internal tube diameter $\boldsymbol{d_{int}}$.[67] We should also mention that dog-bone geometry is not the only possible outcome of radial collapse. In fact, in MWCNT, it has been predicted that the pressure induced radial deformation to collapsed structures can have more than 2 lobes.[54,56,69] In the case of MWCNT in a polymer matrix composite, the 3-lobe collapsed structure has recently been confirmed[68] [Figs. 4(a)–4(d)].

The tube diameter is the critical parameter determining the collapse pressure in SWCNT and MWCNT. For MWCNT, the inter-tube distance is predicted to have also an important effect on collapse pressure.[67] The collapsed nanotube constitutes on its own an interesting nano-object with a hybrid character between a tube and graphene nanoribbon structures. Fully collapsed carbon nanotubes have even been observed at ambient conditions early after the discovery of carbon nanotubes. This is only the case for large diameter tubes (several nm). Such collapsed structures can be critical in many cases as in metal contacts.[73] The physical properties of the pressure collapsed nanosystem are not well known

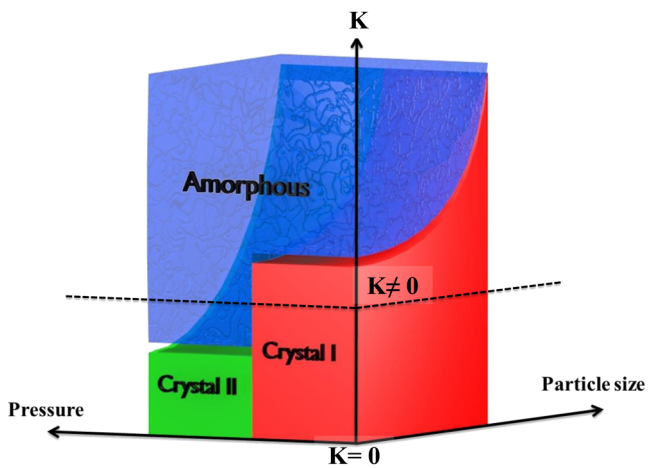

FIG. 3. Multidimensional plot (pressure, particle size, K). The K factor corresponds to the Ginzburg term illustrating the effect of inhomogeneities such as defects, interface, and pressure gradient.

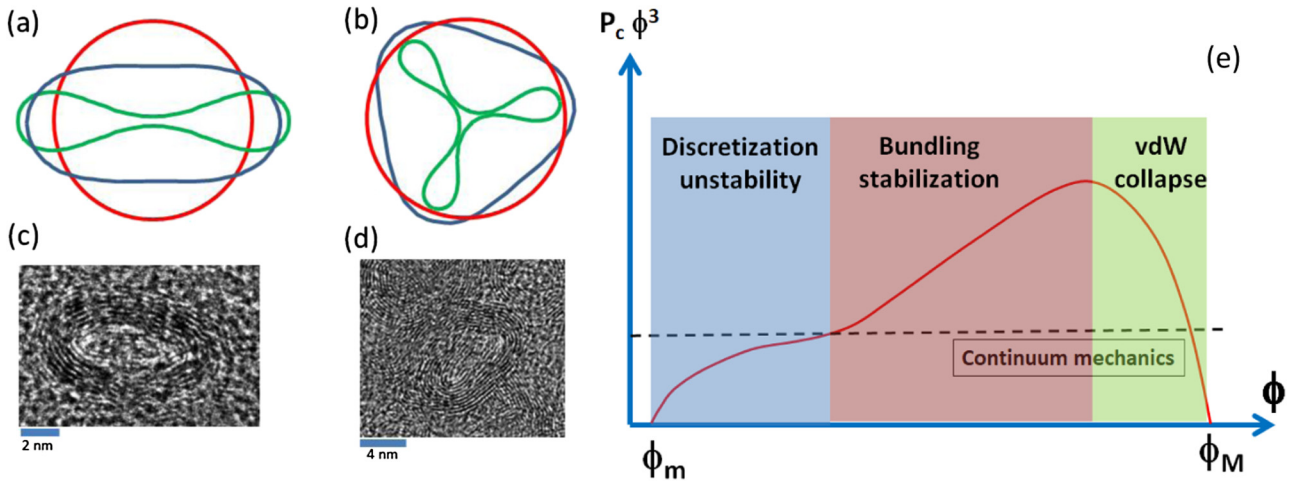

FIG. 4. Pressure induced radial collapse in carbon nanotubes. (a) and (b) depict the calculated evolution of a carbon nanotube cross section in the case of 2 and 3 lobes instability, respectively (adapted from Ref. 69). The ambient pressure configuration (red line) evolves toward the collapsed form (green) going through different structural transformations. In blue, the limiting structure separating positive curvature from negative curvature radius. This last configuration exhibits the flattest regions. (c) and (d) show HRTEM images of MWCNT in a polyamide matrix after a pressure cycle up to 5 GPa[68] where structures close to the limit cross sections in (a) and (b) (blue curves) are observed. (e) Proposed dependence of the normalized collapse pressure (Pc ϕ^3) of SWCNT bundles as a function of tube diameter (ϕ) (red line). The straight dotted line corresponds to the prediction of the continuum mechanics modeling which corresponds with the Lévy-Carrier law. The nanotube evolution includes 3 regimes (see text) evidenced by the colored zones with ϕ_m and ϕ_M being respectively the lowest and highest tube diameters allowing for a stable SWCNT with a circular cross section.

even if some experimental and theoretical investigations seem to point out that its electronic properties may show a strong dependence on chirality and that it may differ from the pristine structure.[74] High pressure modulation of the nanotube radial cross section offers then interesting perspectives for the development of strain-dependent structures with engineered band-structures.

It is also important to consider the changes taking place on carbon nanotube properties during the compression before their radial cross section collapse takes place. First of all, we may note that modeling predicts that individual carbon nanotubes are low compressibility systems with a bulk modulus (inverse of compressibility), B_0, of 230 GPa (pressure derivative $B' = 4.5$) for tubes 0.8 nm in diameter.[75] It is interesting to note that such bulk modulus will be diameter dependent, as it includes the empty volume inside the tube. During the homothetic compression of carbon nanotubes (i.e., without modifying the shape nor the geometrical proportions of the nanotube), strong changes of their excitonic or electronic gaps, E_{ii}, have been predicted[76] and measured.[77,78] Calculations also find a strong variation of the pressure dependence of E_{ii} with tube chirality[76] which can differ even in sign depending on the tube chirality. Such prediction of a geometrical pressure effect on the electronic properties of a nano-object has not been experimentally confirmed as the dielectric screening of the pressure dependent PTM complicates interpretation.

IV. INTERACTION WITH THE NANOMATERIAL ENVIRONMENT

A. Nanocrystals

In nanocrystals, the fraction of atoms at the surface increases as $1/r$ with r being the radius of the nanoparticle. With small nanoparticles, adsorption of surrounding atoms or molecules may modify the surface energy leading to impact the phase stability as discussed in Sec. III A. However, one may wonder whether this effect is similar to all nanomaterials or if some samples may be more influenced than others.

In the case of Y_2O_3, the storage conditions have been shown to have drastic effects on the phase stability. In contact with ambient atmosphere, CO_2 molecules adsorb at the surface and react through the Lux–Flood acid–base reaction to form carbonates. This reaction induces oxygen defects at the surface. The high-pressure transformations are strongly influenced by these defects leading to size-dependent pressure-induced amorphization. In comparison, particles from the same batch but stored under argon atmosphere do not exhibit any signature of carbonates and their pressure-induced transition sequence differs from the carbonated samples.[49] This example illustrates the necessity to consider the specific chemistry of the nanomaterials and the possible reactions with a given environment. A great care should be taken of how the couple sample/environment is chosen.

Mechanical properties of nanomaterials are particularly affected by the effect of the environment and adsorbed species. Because of the reduced size, acoustic vibrations are confined in nanostructures and these low-frequency vibrations may be measured using Raman or Brillouin spectroscopies.[79] Studies under high pressure show that surprisingly these vibrations of individual nano-objects do not couple even under very high pressure.[80] Simulations have demonstrated that the nanoparticles are mechanically isolated thanks to the few water layers that are adsorbed at the surface.[81]

In addition, the studies of the propagation of phonons into a pressurized powder of nanoparticles using Brillouin spectroscopies also indicate that the adsorbed organics play a significant role in the elasticity of a nanopowder. The contact

law between nanoparticles in some cases shows significant deviation from the hard spheres model and should consider the nanoparticles as a hard core-soft shell structure. The effects have a direct implication on the compaction and sintering of nanopowders for high-performance ceramics.[82]

B. Nanotubes

We have already discussed how external isotropic forces induce the radial collapse of carbon nanotubes at critical pressures. Anisotropic forces due to van der Waals interactions can also result in tube radial deformations. In fact, it has been observed the mutual deformation of two carbon nanotubes in contact[83] or the deformation of double-walled carbon nanotubes in contact with a substrate.[84,85] Differences of radial collapse pressure between individual tubes and tubes in bundles[86] and the effect of the PTM on the collapse pressure have been discussed,[82,87,88] but, as we have already pointed out, it is extremely important to make the distinction between the behavior of opened nanotubes which can be invaded by the PTM from those which are closed and then preserved from such modification. In fact, not only the radial deformation will be different between filled and empty tubes, but the pressure collapse can be enhanced by many-fold factors.[78,89] Obviously, the sketched curve in Fig. 4(e) will be strongly modified by nanotube filling. Recent studies point out that, once the non-filling by the PTM of carbon nanotubes is guaranteed, there is a marginal effect of the PTM on the value of the collapse pressure[66] in the absence of chemical reactions and of hydrostaticity effects.

The controlled environment of carbon nanotubes can be also an opportunity for the synthesis of new nanomaterials. We can distinguish the case in which the environment is constituted by other nanotubes or another system. In the first case, opportunities for carbon sp^2 to sp^3 evolution should be considered. It has been shown that both bundles of SWCNT[90] and MWCNT can be transformed to diamond. Such transformation seems to be preceded by the nanotube graphitization[90] which may include tube unzipping or shortening as it has been observed in shock experiments.[91] More interestingly, it has been predicted that sp^3 polymerization between nanotubes in a bundle could lead to the formation of zeolite-type structures.[92] As already discussed in Sec. III B, in the case of MWCNT composites, pressure has been used to modify the radial geometry of the embedded tubes which induced a significant improvement of the electrical conductivity of the composite.[68]

C. Fullerenes

The case of fullerenes is a very interesting example of how the combination of size, topology, and high pressure and/or temperature can become a powerful method to induce new physico-chemical properties in materials. As other non-saturated molecules, fullerenes, with a large variety of configurations such as C_{20}, C_{36}, C_{60}, or C_{70}, polymerise under HP-HT. The most common fullerene, C_{60}, is highly incompressible, but the intermolecular interactions are weak and, under compression, the formation of Carbon-Carbon bonds between the molecules makes it possible to generate polymerized phases. Theoretical calculations[93] suggest that the intermolecular interaction increases with increasing pressure, and at some critical intermolecular distance a sp^3-hybridized covalent C-C bond may be formed. The new polymerised phases usually present crystalline order and they can be recovered at ambient conditions. Up to now, and depending on pressure and temperature synthesis conditions, 1D, 2D, and 3D-C_{60} polymers have been obtained (reviews on this topic in Refs. 94–98). The new polymer phases present lower lattice symmetry than the crystal based on C_{60} monomers, which has, at room temperature, a face centred cubic structure. The low dimension character of these polymerised phases implies that the polymerisation process takes place along some preferred directions. The big challenge is to successfully prepare a crystalline carbon compound having a 3D network similar to silicon clathrate superconductors (see Sec. V B). Promisingly, at HP-HT conditions, C_{60} has been seen to transform into 3D polymer electrically conductive and with hardness comparable to that of cubic boron nitride (BN)[99,100] or into amorphous fullerite phases.[97] Some amorphous phases show ultra-hardness as they can even break diamonds. Cold compression of C_{60}s results in an amorphization of the material above 20 GPa and no 3D superhard phase has been observed unless using a catalyst.[101] The pressure-induced amorphization is irreversible.[102,103] The high pressure treatment seems to trigger a gradual destruction of C_{60} molecules above 10 GPa, and thus amorphization occurs well before the hypothetical 3D polymerization.[103] It was expected that C_{60}, a semiconductor with a bandgap of 1.7 eV, becomes metallic under high pressure and that metallization could occur at around 33 GPa.[104] Though, the molecules collapse at pressures >20 GPa render metallization of pure fullerite unreachable.

C_{70} is much less reactive and has more topo-chemical constraints than C_{60}. For these reasons, the creation of intermolecular bonds in C_{70} is more difficult resulting in slower formation of oligomers and polymers under HP-HT conditions.[105] However, at pressure-temperature conditions similar to those of C_{60} ordered polymerized forms of C_{70} have been found.[106,107]

D. 2D-systems

A new family of nanomaterials has come recently into scene: 2D materials. Because of their structure, the surface is predominant and the majority of atoms—or even all—are in interaction with their surroundings. In graphene, all atoms are surface atoms whereas in transition metal dichalcogenides or in tri-layered graphene a layer of atoms is intercalated between two surfaces. 2D materials are usually grown on surfaces or deposited on a substrate through different methods. High pressure methods constitute a privileged technique to probe the interactions between the 2D-system and the substrate. 2D-systems exhibit also an outstanding stretchability, i.e., the ability to sustain high strain rates without failure which opens new opportunities unattainable for bulk materials. This allows us anticipating huge effects on physical properties. In fact, the accessible strains in 2D systems are one order of magnitude higher than in 3D materials.

However, if the strain transmission in 3D materials is well understood using the continuum mechanics laws, these laws fail for 2D materials. Let us consider the case of pressure which is a force divided by a surface: how pressure can be defined and transmitted laterally on a sample that shows an atomic thickness and for which the concept of surface is irrelevant? To explain such seeming paradox, it is reasonable to assume that the stresses are transmitted through the substrate deformation.

How is the strain transferred between the substrate and the deposited 2D material is a challenging question that is important to answer before using stress as a control parameter of the 2D physical properties.

Several experimental works report the effect of high-pressure on Raman or photoluminescence spectra for several 2D materials.[20,21,108–112] In most high-pressure studies, physical properties (phonons, bandgap, etc.) versus pressure are represented as if pressure was totally transferred to the 2D samples. However, several works have shown that this is not the case and that the substrate compression plays a fundamental role. This is well evidenced by the different pressure dependence of the Raman peaks as a function of the substrate on which the 2D material (graphene in this case) is deposited.[112]

Instead of assuming a total transfer of the applied pressure (measured by the ruby fluorescence technique), one may formulate another hypothesis. This one is based on the fact that the G-mode of graphene measured by Raman spectroscopy is the signature of the C-C stretching vibration. Therefore, its pressure-induced evolution should not depend on the substrate if pressure was totally transmitted. To explain such dependence, one could assume that the strain is (partially) transmitted from the substrate (deformed by pressure) to the 2D materials leading to $\varepsilon_{2D} = \alpha.\varepsilon_{substrate}$ where ε_i is the strain in the 2D sample and in the substrate, respectively, and α is the strain transfer function. Considering the bond scale, one considers the linear compressibility of both the 2D materials (β_{2D}) and the substrate (β_S), which leads to $\alpha \cdot \beta_S \cdot P = \beta_{2D} \cdot \sigma$ where σ is the stress transmitted by the deformation of the substrate. This point is important as it appears that in the case of strain transmission the stress *is not* equal to the pressure. It implies that plotting the Raman shift as a function of pressure is not adapted, the relevant parameter being the induced stress $\sigma = \alpha \cdot (\beta_S/\beta_{2D}) \cdot P$. The obtained value of α depends on the nature of the substrate and is more important for substrates having a higher compressibility (a lower bulk modulus). This can be understood as a consequence of the impossibility—energetically speaking—of graphene to attain the compression imposed by the substrate, which will lead to the realization of a buckling field.

The pressure-dependence of the G-mode of graphene not only depends on the nature of the substrate. It has been shown to also depend on the number of graphene layers deposited on Si/SiO_2 substrate (300 nm of SiO_2 on bulk Si).[20] In the case of mono- and bi-layers, the slope $\partial\omega_G/\partial P$ is higher than tri- and multi-layers. Typically, the slope is around 8 cm^{-1} GPa^{-1} for graphene and bilayer whereas it is close to the value found in graphite (~4.3 cm^{-1} GPa^{-1}) for tri-layers and more layers. Such observation is explained when considering graphene as a membrane in adhesion with the substrate. As already explained, pressure is not directly transmitted to the 2D material but biaxial strain is transmitted through the substrate. This is the case for single-layer and bilayer graphene. In this case, as Si/SiO_2 is highly compressible, it leads to a huge induced biaxial stresses σ, the C-C bond cannot cope, the dragging effect is only partial ($\alpha \neq 1$) and slipping phenomena can occur. A calculation taking into account the competition between the adhesion energy (gain) and bending energy (cost) shows that the unbinding between a graphene stacking and a Si/SiO_2 substrate occurs for a number of layers higher than two. Therefore, strain cannot be transmitted anymore through the substrate deformation. For a trilayer, the pressure is then directly transmitted to the sample by the pressure transmitting medium. An attempt to evaluate both strain and doping effects in graphene from its Raman signature has also been carried on.[113]

A similar study has been performed on MoS_2 supported on Si/SiO_2.[111] In that case, the higher bending modulus of monolayer MoS_2 with respect to graphene allowed evidencing the presence of a bimodal adhesion configuration of monolayer and bilayer MoS_2. In fact, both samples presented a splitting of their Raman modes which was further evidenced with pressure application. The differences of pressure slopes of the two components could be interpreted in terms of two different regions having low and high conformation to the substrate, respectively. Such a scheme disappeared for MoS_2 samples having three or more layers, as observed in graphene.

V. INTERCALATION AND NANO-INSERTION

In many cases, the nature of nano-objects and/or of their mutual interactions is particularly suited either for the intercalation of atoms and molecules or for what we can refer as nano-insertion, a process that, unlike intercalation, does not include electrical charge exchange. This is, in particular, the case of fullerenes or nanotubes—or the corresponding materials made of their assembling—which accept either endohedral and exohedral intercalation or nano-insertion. These possibilities are illustrated in Fig 5 in the general case of nano-caged systems which include also the case of covalent clathrates. Pressure application leads to a reinforcement of the interaction between guest and host species, opening opportunities for the development of new materials or for the fine-tuning of physico-chemical properties. We will discuss these different aspects in the case of fullerenes, clathrates, and nanotubes.

A. Fullerenes

The vast amount of void space in fullerite crystals, along with their cage-like structure (Fig. 5), makes them suitable for intercalation and endohedral doping procedures, allowing for further tuning of their properties. Insertion of metal atoms into the fullerite lattice leads the electron transfer and sometimes the formation of fullerene polymers already at ambient conditions, as it is the case for Na/Li intercalation. In particular, intercalation of alkali-metal atoms in solid C_{60} results in

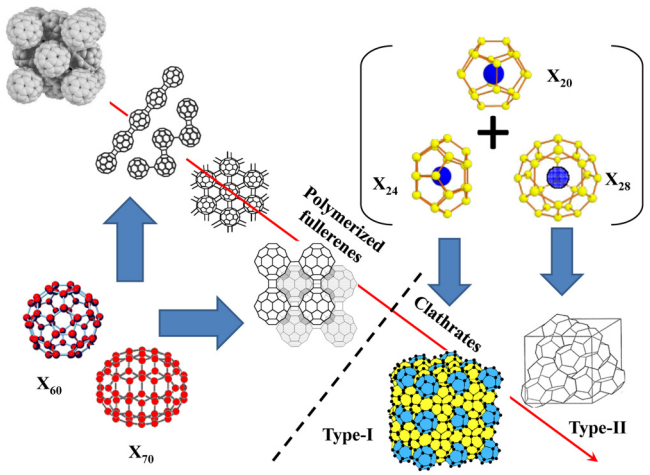

FIG. 5. Representation of different caged nanostructures allowing for various forms of intercalation. The parent molecular structures are represented with the symbol X_n with n = 20, 24, 28, 60, and 70 as examples. The diagonal red arrow shows structures exhibiting progressively stronger and higher number of bonds between the polyhedra. The dashed line distinguishes those structures in which the nanocages are assembled through bonds (fullerites) and those in which the polyhedron merge sharing faces (clathrates). Such clathrate structures cannot be synthesized from their parent polyhedra and they have been then placed between brackets to underline this fact. 1D, 2D, and 3D polymerized fullerenes can be obtained from the van der Waals structure at the top-left corner of the graph.

metallic behavior,[114] and the M_3C_{60} (with M alkali metal) compounds were observed to be superconducting with critical temperature as high as 33 K for $RbCs_2C_{60}$[115] and 40 K for Cs_3C_{60}.[116] Interestingly, Cs_3C_{60} is an insulator at normal pressure but it shows superconductivity at high pressure. Due to the large size of Cs, at ambient conditions, the space between C_{60} is too big and the electrons are held around the C_{60} molecules. When pressure is applied, the intermolecular distances shorten and electrons become delocalized rendering Cs_3C_{60} metallic and exhibiting, at the same time, superconductivity with high Tc. Moreover, as we have previously discussed for pure fullerenes, pressure can induce polymerization opening the way to a variety of incoming novel structures. *Ab initio* calculations on the energetic and structural properties of hypothetical carbon-based cage-like materials suggest the possibility of synthesizing Li-doped carbon clathrate under extreme conditions of pressure and temperature. This potential 3D polymeric Li intercalated fulleride, constituting an alternative to carbon clathrates of type-I or type-II structure (see later), may exhibit excellent mechanical properties and high Tc due to a very high phonon-electron coupling.[117]

Experimentally, one of the interesting effects of alkali intercalations is that, under cold compression, it stabilizes the M_xC_{60} systems to much higher pressures than those reported for pristine form of C_{60} (~18–25 GPa), preserving the molecular integrity of C_{60} molecules. For example, the monomeric structure of Cs_6C_{60} is stable up to 45 GPa[118] while Rb_6C_{60} shows a structural transition to a two-dimensional (2D) polymeric structure above 35 GPa and 600 K.[119] This difference is probably due to the smaller ionic radius of Rb atoms compared to Cs, which allows C_{60} to get close enough to polymerize under high compression. By compressing 2D-Na_4C_{60} and 2D-Li_4C_{60} polymers, it is possible to synthesize low compressible 3D polymeric fullerides through the random creation of new polymeric bonds between fullerene molecules at room temperature and low pressure compared to the higher temperature and pressure needed to achieve 3D polymeric pure C_{60}.[120,121]

Another achievement with alkali intercalated fullerenes has been to use high pressure to obtain higher alkali insertion rates, leading to superdense structures. For pressurized pure or mixed alkali intercalated systems, filling rates 2 to 3 times higher than those for non-pressure intercalated graphites or fullerites were reached. A_xC_{60} compounds with x = 10–16 for A = Na or x = 12–20 for A = Li were obtained. For these, fullerenes were compressed in an alkali-rich environment and submitted to HP-HT. These superdense alkali metal carbon intercalated systems exhibited unusual valence states showing enhanced p- and d-states in chemical bonding. For a review on superdense alkali pressure intercalated carbons, see Ref. 122.

When fullerenes are intercalated with solvents they can generate solvates. C_{60} and C_{70} have been observed to form solvates with almost all common solvents. New interesting phenomena, which have never been observed in pure or alkali intercalated fullerene, appear when studying these compounds under high-pressure conditions. It has been observed, for example, that pressure (i) decreases the transition temperature Tc for the organic ferromagnetic TDAE-C_{60} [TDAE holds for tetrakis(dimethylamino)ethylene, $C_2N_4(CH_3)_8$],[123] (ii) favors orientational ordering transition for C_{60}*C_8H_8 at 0.8 GPa,[124] (iii) induces charge transfer transition in donor-acceptor complexes, as well as polymerization at relatively low pressure (<1 GPa) and room temperature[125] (for a review on the subject, see Ref. 126). Applying high pressure >60 GPa to C_{60}/m-xylene, it is possible to produce a superhard carbon phase composed of ordered amorphous carbon clusters (OACCs).[127] Such formed OACC phase has a long range periodic structure and seems to be the first crystalline material made with amorphous building blocks. Yao *et al.* further emphasize the important role of intercalated solvent (m-xylene) that acts as a spacer to preserve the stability of deformed or collapsed C_{60} molecules and allow their polymerization at higher pressure. The material loses its long-range periodicity if the solvent is evaporated by high temperature treatment.[128] Recently, by applying HP-HT to a bilayer structural solvate, Pei *et al.* were able to generate a unique quasi-3D C_{60} polymer.[129] Another interesting approach is to explore the high pressure transformations of combined co-crystals obtained from fullerenes. This has been recently done by compressing C_8H_8/C_{60} co-crystals up to 45 GPa with the formation of a new type of ordered amorphous system whose final structure could be tuned by varying the compression application time.[130]

The possibility to encapsulate one or more metal atoms inside fullerene cages (endohedral metallofullerenes) could give rise to new species or materials with novel properties. Recently, endohedral fullerenes such as Sc@C_{82}, Y@C_{82}, La@C_{82}, Gd@C_{82}, La_2@C_{80}, and Sc_2@C_{84} have been synthesized in large quantities.[131] Noble gases, such as He and Ar, have also been incorporated in fullerene cages under high

temperature (600 °C-1000 °C) and pressures (~0.3 GPa).[132] Molecular dynamics calculations showed that a H_2 molecule remains stable in a C_{60} cage at 298 K and 0.1 MPa and that pressures over 5 MPa are needed to store H_2 molecules in the C_{60} cage.[133] The behavior of endohedral metallo-fullerenes or non-metal doped fullerenes has not been explored much under pressure. Pioneering works show some promising results for quantum computing such as the application of high pressure seems to improve the thermal stability of spin active endohedral fullerenes encapsulating single nitrogen atoms ($N@C_{60}$ and $N@C_{70}$) at high temperatures.[134]

B. Clathrates

Clathrates can be considered as crystalline structural variants of zeolitic architectures having relatively small voids. They can be viewed as framework structures obtained by the face-sharing assembly of the [5^{12}] pentagonal dodecahedron X_{20} nanocages combined with other polyhedral ones which should include one or more hexagonal faces. The symbol X can represent atoms from the group-IV elements (Si, Ge, Sn), molecules as water or groups as SiO_2. In these cases, we will speak of group-IV clathrates, clathrate hydrates, or clathrasils, respectively. The clathrate nanostructure assemblage description here proposed must be considered somehow virtual as the real synthesis process does not correspond to such bottom-up process. Nevertheless, we will consider the particular case of zeolitic structures without oxygen, both because they constitute a very simple example of nano-intercalation in which high pressure studies have revealed interesting phenomena and in relation to a case of small fullerites with full 3D-polymerization. The introduction of guest species in the nano-caged clathrate structures is in fact at the heart of its own synthesis process. Atoms or molecules, filling space with the highest compacity (i.e., with the minimum empty space per atom), become structure directing agents, constraining the framework organization to minimum energy polyhedral structures.

Applying HP-HT is one of the common routes for the synthesis of group-IV clathrates[135,136] and sometimes for the synthesis of new clathrate hydrates.[137] Clathrasils are mostly synthesized using hydrothermal methods[138] which is also the natural process for the formation of clathrate hydrates.

Different families of clathrates have been investigated as potential materials for carbon dioxide sequestration, hydrogen or natural gas storage and transportation[139] or Li-ion batteries. HP-HT synthesized clathrates are also studied for the development of new thermoelectric materials and novel superconductors. The clathrate structure appears in fact as very favorable for superconductivity. The high pressure robustness of superconductivity in silicon clathrate structures has recently been shown in Ba_8Si_{46},[140] and predictions for high critical temperature superconductivity of high pressure stabilized hydride clathrate structures such as CaH_6[141] or YH_6[142] reinforce such idea. Carbon clathrates are also predicted as candidates for very high T_c superconductivity.[143] Nevertheless, even if carbon clathrate synthesis seems to be not too favorable from the thermodynamic point of view,[71] the recently synthesized B-C framework mixed clathrates[144] could appear as a promising alternative system to explore clathrate high Tc superconductivity.

Group-IV clathrates are also extensively explored for thermoelectric applications.[145] In the guest-host system, the coupling of more localized phonons, involving guests, with the framework ones leads to important heat transport reduction whereas intercalation plus metallic substitution in the framework structure, allows for a fine-tuning of carrier concentration and for band structure engineering. In this way, clathrates appear as parametric materials for the optimization of the ZT thermoelectric efficiency parameter [the ZT figure of merit is defined as $ZT = (S^2\,\sigma/\kappa)T$ where S is the Seebeck coefficient, σ is the electrical conductivity, and κ is the thermal conductivity, with T being the temperature].

HP-HT application has been successful in the synthesis of a number of clathrate materials including silicon superconducting clathrates as Ba_8Si_{46}[146] and other related structures,[147,148] $Ba_{8-x}Sr_xSi_{46}$,[149] tellurium-mixed clathrates,[150] or iodine-mixed clathrates.[151] LVP devices such as multi-anvil cells or belt-apparatus were generally used. Most of the obtained samples are polycrystalline, but small single crystal can be also isolated in some cases.[152]

The high pressure phase diagrams of silicon clathrates of different types have been extensively studied. First, it has been shown that the pressure stability of guest free silicon clathrates is very closely related to the phase diagram of silicon in the diamond structure.[153] Secondly, that phase diagram can be strongly modified when considering nanocage filling with different atomic species. In most cases, atomic filling leads to a first phase transition in the form of volume collapse followed by a structural amorphization.[154] On pressure release, it has been observed a polyamorphic transformation into a lower density phase.[155] The nature of the volume collapse transition is still widely debated.[156]

C. Nanotubes

Nanotubes, like fullerenes, allow for exohedral and endohedral insertion or intercalation of atomic or molecular species. This may allow obtaining and tuning the electrical conductivity of the system with different degrees of donor or acceptor intercalation. As in the case of fullerenes, high pressure has also been used to reach higher filling rates of alkali metals. This was the case for lithium intercalation in MWCNTs for which filling ratios of 1–2 Lithium atoms for Carbon atom were reached with pressures of 4.5 to 6 GPa at 300 °C.[157]

As already discussed, pressure application in empty nanotubes leads to a modification of the nanotube cross section through an ovalization/collapse process. Endohedral intercalation/insertion can lead, in a similar way to the clathrate case, to the stabilization of the pristine structure at much higher pressures. This has been demonstrated in the case of water[66,85] or CO_2[89] filling, iodine intercalation,[158] carbyne[159] or C_{70} filling[160] of SWCNTs. The effect can be huge, with a full collapse pressure going from 3.8 GPa for the pristine (empty) sample to ~17 GPa in the case of the water filling of the same 1.32 ± 0.08 nm diameter SWCNTs.[78] For similar diameters and argon filling, the same type of tubes did not show a clear sign of collapse up to pressures of 40 GPa.[161]

We may underline that before the 2015 work of Torres-Dias *et al.*,[78] most experimental high pressure studies did not consider the filling of carbon nanotubes by the pressure transmitting media. This led to an important confusion in the scientific literature with articles claiming transition pressures in the 10–20 GPa domain while others claimed, for the same nanotube diameter range, collapse pressures in the GPa range. These two cases corresponded to PTM filled opened tubes and to empty closed tubes, respectively. Of course, due to steric effects, we cannot expect similar geometrical changes in the nanotube cross sections for empty and filled tubes.[89]

Another important aspect of endohedral insertion or intercalation of carbon nanotubes is that carbon nanotubes act as real nano-anvils during the collapse process. They constitute a tunable 1D-volume with pressure allowing studying the effect of the geometrical or tube cross section changes on the structure and properties of the nanoconfined species. In that way, it has been shown by Density Functional Theory (DFT) calculations that water or CO_2 inside SWCNT can form different types of structures at nanotube collapse depending on the nanotube filling ratio including 1D molecular chains, 2D nanoribbons, and even molecular single and multi-walled nanotubes.[89] The bonding scheme of molecular systems can be also modified inside carbon nanotubes. This has been first shown in the so-called peapods (fullerene filled nanotubes) for which it is possible to polymerize the C60 chain through HP-HT treatment.[162–166] Halogen spiral chains formed inside carbon nanotubes have been modified by pressure application as it has been shown in iodine endohedrally intercalated nanotubes. The nanotube ovalization leads to a progressive linearization of the iodine polyanions and a reduction of charged species on pressure release.[158] In the case of exohedrally bromine intercalated double-walled carbon nanotubes,[167] the pressure, inducing collapse of the structure at 15 GPa, leads to significant reversible modifications of the poly-ionic structuration of bromine. Evidence of an irreversible cross-linking between the carbon chains inside carbon nanotubes and the wall of the inner tube, it has been shown after a pressure cycle up to 39 GPa in filled DWCNT collapsing at ~13 GPa.[159] This evolution involves then the formation of a new carbon nanomaterial including an evolution from sp to sp^2 hybridization of the C atoms of the carbyne chain and from sp^2 to sp^3 hybridization for some atoms of the nanotube structure. Compression of ferrocene filled SWCNT[168] leads to the increase of host–guest interactions with a decomposition of the ferrocene molecules. The authors also propose the formation of a new 3D zeolite-like structure from the nanotube interlink, which is quenchable to ambient conditions. Also, graphene nanoribbon analogues made of polymerized perylene molecules filling SWCNTs have been studied under high pressure.[169]

VI. PERSPECTIVES AND POTENTIAL APPLICATIONS

In this section, we will list the different opportunities that high pressure applied on nanomaterials can offer for the synthesis of new phases in view of potential applications. We will first analyze some general aspects about phase metastability and then we will concentrate on the specific techniques of new material synthesis. We will first consider some novel techniques such as HP-HT synthesis of nano-sized polycrystalline hard materials or sintering at the nanoscale. Then, we will discuss other much less exploited high pressure synthesis methods, such as polymerization of nanostructures, bending/folding of nanostructures, breaking of nanostructures, or interaction with the PTM. We will finally consider progress in the study of individual nano-objects at high pressure. In our opinion, this kind of study will strongly develop in the forthcoming years and will lead, in combination with theoretical methods, to advanced high pressure engineering of nanosystems.

A. High pressure metastability

Presently, there are few applications of high pressure in the production of new materials or nanomaterials. Historically, high pressure synthesis has found few real-life applications beyond manufacturing of diamond and diamond-like materials. The major reason for this is the unstable nature of the high pressure phases at ambient conditions. To preserve these high-pressure phases, spinodal limits need to be shifted in order to metastabilize and preserve phases obtained during high-pressure treatment.

Nanostructuration is a way of tuning the thermodynamics of a system that allows modifying the associated energy landscapes and the kinetics of phase transitions on both compression and decompression paths. We may expect in that respect also important future contributions of modeling and theoretical calculations. In fact, until very recently, the theoretical models of thermodynamic paths allowing the metastabilization of high pressure phases have remained elusive. The continuous progress of calculation capabilities and the development of calculation methods let us foresee the introduction of the thermodynamic path as a computing parameter. This should contribute to enhance the predictive capabilities of condensed matter computing, further developing the dialogue between experimentalists and theoreticians.

All in all, it remains true that the sample volume of high pressure phases demanding synthesis conditions at pressures beyond the GPa (or even less) is very small and the produced material needs a high added value in order to comply with the economic constraints of industrial applications. This is particularly the case for the high pressure synthesis of diamond. Nevertheless, years after the discovery of the high pressure synthesis, the CVD process has been developed. We may then argue that high pressure synthesis must be explored as a means to obtain and study new materials, which may later be synthesized by other methods if societal or industrial interests are demonstrated. These general considerations also apply to new phases obtained from nanomaterials.

In the following, we discuss different areas or methods in which, in our opinion, nanostructuration or nanosystems should play or continue to play an important role in the future.

B. Ultra-hard nanosized polycrystals

As mentioned earlier, quantum confinement effects in nanosystems lead to different physico-chemical

characteristics with respect to the bulk counterparts as well as different collective physical properties related to nanosize. A good example of this last aspect is the HP-HT synthesis of nano-polycrystalline diamond (NPD) or c-BN (NPcBN) which exhibit superior qualities to single-crystal. The so-called Hall-Petch effect, by particle size reduction, is invoked to explain enhanced mechanical properties both in NPD[5] and in NPcBN.[170] The physical mechanisms associated with such enhancement are still debated and may differ from the Hall-Petch mechanisms in microcrystalline materials. In particular, it appears that new characteristic lengths as those introduced by nano-twinning or defects can play an important role.[170] Nano-Polycrystalline Diamond (NPD) consists of nanometric diamonds densely packed in random orientations. That leads to a mechanical anisotropy and prevents cleavage. Nano-structuration also lowers the thermal conductivity of diamond and this improves its mechanical properties at high temperature. NPD can be easily cut by pulsed laser to various forms, such as anvils for DAC or LVP. They are already in use in some research applications, such as high pressure x-ray spectroscopy studies.[171] In 2012, the Japanese company, Sumitomo Electric, has launched the first tools featuring nano-polycrystalline diamond.

C. Nanosize sintering

Many efforts are devoted to preserve the advantages of the nanoscale properties in macroscopic size materials both in single-phase and in polycrystalline or composite materials. The application of high pressure conditions is explored in some cases as a possible step in the manufacturing of nano-based materials. The full compaction of metallic or ceramic nanopowders could be a powerful mean to produce advanced materials with exceptional mechanical, optical, or thermoelectric properties, for example. The key problem, especially for ceramics, is that high temperatures are required for sintering. Thus, preserving small grain sizes in the 20 ± 10 nm range in a dense material is very challenging as densification and grain growth proceed simultaneously. Furthermore, the smaller the nanoparticles are, the faster the particle coarsening kinetics proceeds. Hot pressing under very high pressure (1 to 25 GPa) using LVP enhances the densification at lower temperatures and gives rise to almost full densification of nanoparticles with a limited grain growth.[172,173] LVPs have shown their efficiency to manufacture fully dense nanoceramics with an excellent optical transparency and higher hardness than microcrystalline ceramics.[174] The remarkable mechanical properties of the poly-nanocrystalline compacts are explained by the nanostructure itself, which prevents the propagation of micro-cracks enhancing fracture toughness. The classical Hall-Petch mechanisms are often invoked in the physical origin of the mechanical properties enhancement, but other mechanisms involving the plastic deformation of nanoparticles are also suggested.[175,176] In addition to grain nanosize preservation, high pressure sintering has the great advantage to stabilize high pressure metastable phases such as cubic boron nitride (cBN), diamond, or stishovite. Ultra-hard poly-nanocrystalline cBN,[170,177] nano-diamond,[5] stishovite[178] compacts are elaborated in LVP by the HP-HT transformation of precursor systems as already discussed in Sec. VI B. Unfortunately, pressures as high as 20 GPa are required. The use of very high pressure LVP in nanoceramic processing then remains a niche route. A more widely used technique is the Spark Plasma Sintering (SPS), a hot pressing technique where very high heating rates (up to 1000 °C/min) are achieved by application of high intensity pulsed electrical current, leading to super-fast densification of nanopowders (within few minutes). Despite the short sintering time, SPS does not allow to preserve the original nanograin size at full densification. Combination of high pressure and high heating rate might be the key allowing to optimize the synthesis of dense nanoparticles compacts with about 10 nm grain size.[179] The usual pressure range used in SPS is limited to 150 MPa by the compressive strength of graphite dies. Nevertheless, SPS high pressure devices have recently been developed to reach 1 GPa[179] to 10 GPa.[180–182] This opens a new field for the design of advanced materials that will benefit from the properties of nanoparticles.

D. Bonding/Polymerization of nano-objects

We have mentioned the countless possibilities in engineering new materials by combining topology, assembly, endohedral inclusions, or intercalation with high pressure. The possibilities offered by the 1D, 2D, or 3D polymerization of C_{60} have been extensively explored and discussed in Sec. IV C. More studies on C_{70} and derivatives at high pressure could be very interesting as the directional bonding properties of C_{70} molecules could enable the creation of anisotropic structures with novel properties.

We have also discussed in Sec. IV B the possibilities for new material synthesis offered by the high pressure covalent bonding between carbon nanotubes. Different modeling studies tend to confirm that possible scenario. The formation of new nanostructures through sp^3 bonding of carbon nanotubes have been in fact predicted for small diameter carbon nanotubes.[183,184] Today, the experimental limitations avoiding the controlled high pressure polymerization of carbon nanotubes arise from the sample purity. In fact, pure bundles of carbon nanotubes composed of nanotubes of the same chirality are not yet available without the presence of surfactant or polymer molecules. Many progresses done in recent years toward the chiral purification of carbon nanotubes let us envisage the possible development of such new type of nanopolymers in the near future.

The same "bonding strategy" may apply to 2D systems. We may underline in that respect the recent announcement of the high pressure synthesis of "diamondene,"[185] a proposed 2D-system made of sp^3 carbon obtained via the pressure-induced bonding between the two planes of a bilayer graphene system.

E. Bending and deforming nanostructures

The topology of certain nanostructures favors very low bending rigidity in certain directions. This is the case in nanotube structures in the radial direction or in 2D systems in the direction perpendicular to the plane. Pressure application can allow setting strategies to tune in different ways the

geometry of such structures by bending. As discussed in Sec. III B when considering size effects in carbon nanotubes, there are limiting values for CNT stability as a function of their size. In particular, for large SWCNTs, a reversible transition toward dog-bone cross sections can be reached with very moderate pressures. Bending of nanotubes can lead to very important changes in their physico-chemical properties such as semiconductor to metal or metal to semiconductor transitions (see, for instance, Ref. 68 for a discussion on carbon nanotubes and Ref. 186 for BN nanotubes). Another interesting aspect is that nanotube deformation can also allow for strong interactions with active molecules introduced inside the nanotube (see Sec. V C). We could then expect the use of large carbon nanotubes in active switching devices or composites or as sensors.[187] Further investigations, both experimental and theoretical, would be needed to explore these possibilities, including the characterization of individual carbon nanotubes under high pressure. Again industrial applications will imply the selection or growing of selected large diameter carbon nanotubes, which appears presently more challenging than for low diameter (<1 nm for SWCNT) tubes.

An interesting class of materials which could permit exploiting the radial deformation of carbon nanostructures is nanocomposite. Carbon nanotubes can be incorporated in different matrices, especially polymeric, in order to enhance the mechanical or electrical properties of the final material. In particular, the possibilities to use such types of composites as pressure sensors are explored. The softness of the matrix should allow a modification of the electrical conductivity of the percolated nanotube network. In the case of MWCNT composites, a pressure of 1–5 GPa has been used to modify the radial geometry of the embedded tubes in a polymer matrix with an *in situ* significant reduction of the electrical resistivity of the composite[68] which is attributed to an improvement of the electrical contact between carbon nanotubes. A permanent pressure-induced radial deformation of the tube—stabilized through some local polymer densification—was observed by electron microscopy (Fig. 4).

High pressure deformation in atomic-thick-like 2D systems is an emerging area. In fact, it has been recently shown that supported 2D structures under high pressure follow a strong biaxial strain due to the volume reduction of the supporting substrate as was discussed in Sec. IV D. When the substrate surface is much more compressible than the in-layer bonds of the 2D system, this last one tends to bend or wrinkle and a limited strain transfer is then detected.[112] An engineered substrate supporting the 2D-system could allow the control of such deformations patterning. This can offer new opportunities for the development of pressure switching devices under different stress conditions.

Coupled to micro- and nano-technology fabrication methods, the development of NEMS (Nano Electro-Mechanical Systems) or sensors based on pressure or strain deformed nano-objects constitutes also an interesting route of research.[188] Based on the significant modifications observed in the electronic properties of 1D and 2D nanomaterials under different strain conditions, straintronic is a domain that will certainly benefit from the exploration of the high pressure domain.

F. Breaking nanostructures

The use of mechanical constraints to reduce the size of microcrystals to reach nanoparticle dimensions is in use since many decades in techniques such as ball milling or Severe Plastic Deformation (SPD). Ball milling uses ball impact and attrition to reduce particle size (see, for instance, Ref. 189 for a review) whereas SPD combines high hydrostatic pressure with large shear strain in different techniques such as equal-channel angular pressing, high pressure torsion, or asymmetric rolling (see Ref. 190 for a review). In both cases, large local strains in the GPa or multi-GPa regime can be reached. Even if crystalline phase transformations or amorphization processes have sometimes been reported in particular for ball milling,[191] these techniques do not usually involve phase transformations but they are particularly important for industrial applications.

Breaking nanostructures using high hydrostatic pressures has also been used. The irreversible graphitization of carbon nanotubes following radial collapse has been reported for SWCNT in combined HP-HT experiments (12 GPa, 1500 K).[90] Furthermore, using shock waves in DWCNT, it was shown that pressure above the collapse one was necessary to induce important damage in the nanotubes.[91] It will be important to clarify if such changes are related solely to the collapse pressure or to a given high pressure threshold. In fact, this breaking or unzipping method of carbon nanotubes constitutes an alternative method for graphene nanoribbon production.[192] It is important to understand if such transformation can be reached at moderate pressures for large nanotube diameters having low collapse pressures. The effect of the number of walls and of temperature also needs to be understood.

The collapse of carbon nanotubes offers a unique method for nanostructure breaking acting as nano-anvils. This has been applied in the case of SWCNT filled with fullerenes, the so-called peapods. It was shown that at pressures beyond the collapse pressure, C_{70} fullerenes are destroyed[160] after the radial collapse of the carbon tubes. More recently, it has been shown[193] that the fullerene structure evolves to an amorphous confined chain which may further evolve to a new carbon crystalline form.

G. Taking advantage of the PTM

We have also discussed the high sensitivity of nanostructured systems to their environment which offer certainly many engineering possibilities. In high-pressure experiments, such environment is constituted by the PTM. The choice of the PTM can be done in order to optimize the hydrostatic conditions or to minimize or maximize its interaction with the nanostructures.

In particular, in the case of nanocrystals, the interaction of the environment with surface atoms can contribute to the fine-tuning of phase transformations with the possibility of stabilizing new phases through the modification of the particle surface energy or reactivity. Carbon nanotubes or 2D materials constitute also a fantastic playground for the design

of novel systems and materials. For example, endohedral inserted molecules or atomic systems in nanotubes will be strongly modified by pressure application both through the modulation of their geometrical organization and through density changes. Filling of carbon nanotubes or intercalation in 2D systems modifies both the electronic and the mechanical properties of the system, including a significant enhanced pressure stability. This presents a potential interest in composites and NEMS.

Finally, the coupling of high pressure and solvent intercalation appears to be a powerful strategy to metastabilize hybrid nanostructures such as fullerite materials with unique structures and properties. This seems to be a promising field of research as the possibilities of combining different species of solvent with different architectures are enormous. In the case of fullerites, an interesting challenge will be to apply external pressure to disclose how the properties of endohedral metal or non-metal doped fullerenes are modified in view to metastabilize new polymerized forms that could be promising for quantum technology, for instance, as qubits in spin quantum computers.

H. Individual nanosystems at high pressure

In the forthcoming years, we may expect a significant evolution in the study of individual nanosystems under extreme conditions. The important effects of geometry or size on their physical properties will be tackled with much higher accuracy through the experimental study of well-characterized individual nano-objects, close to idealized systems used in theoretical studies. Up to now, the high pressure experimental study of individual nanosystems has been limited to electronic transport experiments, which are particularly influenced by the electric contact evolution or by the interaction with the supporting substrate.[36,38,188]

Coupling of high pressure devices with the methods of micro- and nano-technologies should certainly play an important role in the high pressure study of individual nanosystems. Optical spectroscopies are particularly well adapted techniques in that view, avoiding side effects as those mentioned in electronic transport experiments. In particular, we may expect important advances using those techniques for which spectroscopic measurement of single individual nano-objects at ambient conditions has already been reached, such as in Raman spectroscopy[194] or Spatial Modulated Spectroscopy (SMS).[85,195]

X-ray synchrotron radiation probes are also well adapted methods for the *in situ* study of individual nano-objects at high pressure which can also be coupled with *ex situ* probes characteristic of nanoscience and surface sciences. In particular, the development of X-ray synchrotron sources including X-ray Free Electron Lasers (XFEL) or the foreseen upgrade of a number of 3rd generation synchrotron facilities will certainly have a significant contribution in such developments, thanks to the concomitant enhanced brilliance and reduction of beam-size. In fact, as well as for optical spectroscopies, first studies of individual nano-objects at ambient pressure have already been developed, in particular, for X-ray diffraction.[196]

VII. CONCLUDING REMARKS

The different physical processes or techniques discussed in Secs. VI A–VI H could be of course combined in different ways, either for the study of nanomaterials at extreme conditions of pressure or for the synthesis of new materials. Breaking, bending, filling, and transforming nano-objects may be considered as different steps of a sequential process, for instance. It may be possible to obtain new diamond doped forms from filled carbon nanotubes. It is in fact possible to obtain diamond doped iodine from the HP-HT transformation of endohedrally iodine filled SWCNT;[90] under pressure the iodine filled tube first radially collapsed, then broke into graphenic-like intercalated system and transformed into diamond.

More generally, we have discussed that pressure allows modifications of the material architecture at different scales, from the crystallographic arrangement to the mesostructure. This opens the opportunity to tune the associated properties combining extreme conditions with nanosized systems of well-controlled size, a terrain which constitutes an avenue for the synthesis of novel nanostructures at different scales. Open opportunities involve the field of nanocomposite materials or NEMS development, fields which will strongly benefit from the continuous development of synthesis or separation methods of monodispersed samples.

Finally, we may then think of nanocrystals, fullerenes, nanotubes, or the different types of 2D systems as the constitutive units for the development of endless types of new materials combining the same type of nano-objects or different types of nano-objects in a final material. Setting the thermodynamic conditions for the mechanisms we have evoked in Subsections VI D to VI F (bonding, bending, breaking) offers never-ending opportunities for the engineering of new materials by controlling the size and geometry of the nano-object. The combined additional opportunities offered by the intercalation or insertion of different atoms or molecules as well as the control of the environment should allow progress in the fine-tuning of physical and chemical properties of the final engineered material. As mentioned, the low sample volume inherent to the high pressure technology is largely compensated by the open opportunities of the newly discovered materials which may be then synthesized following more industrially friendly approaches. Nanomaterials designed with high pressure should then contribute to tackling the different technological and global challenges of our world in the 21st century.

ACKNOWLEDGMENTS

The authors acknowledge support from the iMUST LABEX program MUSCAT-2D. The authors are indebted to Simon Boddy for helping in editing the manuscript.

[1]V. D. Blank and E. I. Estrin, *Phase Transitions in Solids Under High Pressure* (CRC Press, 2013).
[2]D. Machon, F. Meersman, M. C. Wilding, M. Wilson, and P. F. McMillan, Prog. Mater. Sci. **61**, 216 (2014).
[3]A. San-Miguel, Chem. Soc. Rev. **35**, 876 (2006).
[4]G. Mittal, V. Dhand, K. Y. Rhee, S.-J. Park, and W. R. Lee, J. Ind. Eng. Chem. **21**, 11 (2015).

[5]T. Irifune, A. Kurio, S. Sakamoto, T. Inoue, and H. Sumiya, Nature **421**, 599 (2003).
[6]V. Y. Dolmatov, Russ. Chem. Rev. **76**, 339 (2007).
[7]G. Shen and H. K. Mao, Rep. Prog. Phys. **80**, 016101 (2017).
[8]S. Klotz, J.-C. Chervin, P. Munsch, and G. L. Marchand, J. Phys. Appl. Phys. **42**, 075413 (2009).
[9]S. Pasternak, G. Aquilanti, S. Pascarelli, R. Poloni, B. Canny, M.-V. Coulet, and L. Zhang, Rev. Sci. Instrum. **79**, 085103 (2008).
[10]S. Petitgirard, A. Salamat, P. Beck, G. Weck, and P. Bouvier, J. Synchrotron Radiat. **21**, 89 (2013).
[11]J. P. Itie, A. Polian, D. Martinez, V. Briois, A. DiCicco, A. Filipponi, and A. San Miguel, J. Phys. IV France **7**, C2–31 (1997).
[12]S. Le Floch, F. Balima, V. Pischedda, F. Legrand, and A. San-Miguel, Rev. Sci. Instrum. **86**, 023901 (2015).
[13]A. L. Aguiar, E. B. Barros, R. B. Capaz, A. G. Souza Filho, P. T. C. Freire, J. Mendes Filho, D. Machon, C. Caillier, Y. A. Kim, H. Muramatsu, M. Endo, and A. San-Miguel, J. Phys. Chem. C **115**, 5378 (2011).
[14]J. C. Chervin, B. Canny, J. M. Besson, and P. Pruzan, Rev. Sci. Instrum. **66**, 2595 (1995).
[15]N. Chauvin, A. Mavel, G. Patriarche, B. Masenelli, M. Gendry, and D. Machon, Nano Lett. **16**, 2926 (2016).
[16]J. T. B. Salce, A. Demuer, J. J. Blanchard, J. M. Martinod, L. Devoille, and A. Guillaume, Rev. Sci. Instrum. **71**, 2461 (2000).
[17]H. Bureau, M. Burchard, S. Kubsky, S. Henry, C. Gonde, A. Zaitsev, and J. Meijer, High Press. Res. **26**, 251 (2006).
[18]M. Millot, S. George, J.-M. Broto, B. Couzinet, J.-C. Chervin, A. Polian, C. Power, and J. González, High Press. Res. **28**, 627 (2008).
[19]V. V. Shchennikov, S. V. Ovsyannikov, and A. Y. Manakov, J. Phys. Chem. Solids **71**, 1168 (2010).
[20]J. Nicolle, D. Machon, P. Poncharal, O. Pierre-Louis, and A. San-Miguel, Nano Lett. **11**, 3564 (2011).
[21]D. Machon, C. Bousige, R. Alencar, A. Torres-Dias, F. Balima, J. Nicolle, G. de Sousa Pinheiro, A. G. Souza Filho, and A. San-Miguel, J. Raman Spectrosc. **49**, 121 (2018).
[22]P. Toulemonde, C. Goujon, L. Laversenne, P. Bordet, R. Bruyère, M. Legendre, O. Leynaud, A. Prat, and M. Mezouar, High Press. Res. **34**, 167 (2014).
[23]G. Morard, M. Mezouar, N. Rey, R. Poloni, A. Merlen, S. Le Floch, P. Toulemonde, S. Pascarelli, A. San-Miguel, C. Sanloup, and G. Fiquet, High Press. Res. **27**, 223 (2007).
[24]C. Goujon, M. Legendre, P. Plaindoux, A. Prat, and R. Bruyère, High Press. Res. **31**, 375 (2011).
[25]R. Hinrichs and J. A. H. da Jornada, Rev. Sci. Instrum. **68**, 193 (1997).
[26]S. Matityahu, M. Emuna, E. Yahel, G. Makov, and Y. Greenberg, Rev. Sci. Instrum. **86**, 043902 (2015).
[27]M. Gauthier, D. Lheureux, F. Decremps, M. Fischer, J. P. Itié, G. Syfosse, and A. Polian, Rev. Sci. Instrum. **74**, 3712 (2003).
[28]G. Shen and Y. Wang, Rev. Mineral. Geochem. **78**, 745 (2014).
[29]H. T. Hall, Rev. Sci. Instrum. **31**, 125 (1960).
[30]O. Fukunaga, J. Phys. Colloq. **45**, C8–315 (1984).
[31]A. I. Prikhna, J. Superhard Mater. **30**, 1 (2008).
[32]T. Irifune, F. Isobe, and T. Shinmei, Phys. Earth Planet. Inter. **228**, 255 (2014).
[33]D. Yamazaki, E. Ito, T. Yoshino, N. Tsujino, A. Yoneda, X. Guo, F. Xu, Y. Higo, and K. Funakoshi, Phys. Earth Planet. Inter. **228**, 262 (2014).
[34]T. Taniguchi, M. Akaishi, Y. Kanke, and S. Yamaoka, Rev. Sci. Instrum. **75**, 1959 (2004).
[35]E. Colombier and D. Braithwaite, Rev. Sci. Instrum. **78**, 093903 (2007).
[36]C. Caillier, A. Ayari, S. Le Floch, H. Feret, G. Guiraud, and A. San-Miguel, High Press. Res. **31**, 367 (2011).
[37]F. Tomioka, M. Hedo, I. Umehara, T. Ono, Y. Uwatoko, N. Kimura, and S. Takayanagi, J. Magn. Magn. Mater. **310**, 340 (2007).
[38]J.-C. Blancon, A. Ayari, L. Marty, N. Bendiab, and A. San-Miguel, J. Appl. Phys. **114**, 143704 (2013).
[39]S. H. Tolbert and A. P. Alivisatos, Annu. Rev. Phys. Chem. **46**, 595 (1995).
[40]D. Machon, L. Piot, D. Hapiuk, B. Masenelli, F. Demoisson, R. Piolet, M. Ariane, S. Mishra, S. Daniele, M. Hosni, N. Jouini, S. Farhat, and P. Mélinon, Nano Lett. **14**, 269 (2014).
[41]C. C. Yang and Y.-W. Mai, Mater. Sci. Eng. R Rep. **79**, 1 (2014).
[42]S. Li, Z. Wen, and Q. Jiang, Scr. Mater. **59**, 526 (2008).
[43]J. Z. Jiang, J. S. Olsen, L. Gerward, D. Frost, D. Rubie, and J. Peyronneau, Europhys. Lett. **50**, 48 (2000).
[44]R. S. Kumar, A. L. Cornelius, and M. F. Nicol, Curr. Appl. Phys. **7**, 135 (2007).
[45]J. Y. Liang, L. Guo, H. B. Xu, L. Jing, L. X. Dong, W. Z. Hua, W. Z. Yu, and J. Weber, J. Cryst. Growth **252**, 226 (2003).
[46]E. Grzanka, S. Gierlotka, S. Stelmakh, B. Palosz, T. Strachowski, A. Swiderska-Sroda, G. Kalisz, W. Lojkowski, and F. Porsch, in *Ninth European Powder Diffraction Conference 2–5 September 2004* (De Gruyter, Berlin, 2006).
[47]P. Tolédano and U. Bismayer, J. Phys. Condens. Matter **17**, 6627 (2005).
[48]D. Machon and P. Mélinon, Phys. Chem. Chem. Phys. **17**, 903 (2015).
[49]L. Piot, S. Le Floch, T. Cornier, S. Daniele, and D. Machon, J. Phys. Chem. C **117**, 11133 (2013).
[50]D. Machon, M. Daniel, P. Bouvier, S. Daniele, S. Le Floch, P. Melinon, and V. Pischedda, J. Phys. Chem. C **115**, 22286 (2011).
[51]F. Decremps, J. Pellicer-Porres, F. Datchi, J. P. Itié, A. Polian, F. Baudelet, and J. Z. Jiang, Appl. Phys. Lett. **81**, 4820 (2002).
[52]J. Elliott, J. Sandler, A. Windle, R. Young, and M. Shaffer, Phys. Rev. Lett. **92**, 095501 (2004).
[53]P. Tangney, R. B. Capaz, C. D. Spataru, M. L. Cohen, and S. G. Louie, Nano Lett. **5**, 2268 (2005).
[54]H. Shima and M. Sato, Phys. Status Solidi A **206**, 2228 (2009).
[55]N. M. Pugno, J. Mech. Phys. Solids **58**, 1397 (2010).
[56]T. F. T. Cerqueira, S. Botti, A. San-Miguel, and M. A. L. Marques, Carbon **69**, 355 (2014).
[57]A. Sood, P. Teresdesai, D. Muthu, R. Sen, A. Govindaraj, and C. Rao, Phys. Status Solidi B-Basic Res. **215**, 393 (1999).
[58]U. D. Venkateswaran, A. M. Rao, E. Richter, M. Menon, A. Rinzler, R. E. Smalley, and P. C. Eklund, Phys. Rev. B **59**, 10928 (1999).
[59]J. R. Wood, M. D. Frogley, E. R. Meurs, A. D. Prins, T. Peijs, D. J. Dunstan, and H. D. Wagner, J. Phys. Chem. B **103**, 10388 (1999).
[60]M. J. Peters, L. E. McNeil, J. P. Lu, and D. Kahn, Phys. Rev. B **61**, 5939 (2000).
[61]S. Rols, I. N. Goncharenko, R. Almairac, J. L. Sauvajol, and I. Mirebeau, Phys. Rev. B **64**, 153401 (2001).
[62]C. Caillier, D. Machon, A. San-Miguel, R. Arenal, G. Montagnac, H. Cardon, M. Kalbac, M. Zukalova, and L. Kavan, Phys. Rev. B **77**, 125418 (2008).
[63]M. Yao, Z. Wang, B. Liu, Y. Zou, S. Yu, W. Lin, Y. Hou, S. Pan, M. Jin, B. Zou, T. Cui, G. Zou, and B. Sundqvist, Phys. Rev. B **78**, 205411 (2008).
[64]Y. Shen and D. Zerulla, Phys. Rev B **95**, 205434 (2017).
[65]M. Lévy, J. Math. Pures Appl. **10**, 5 (1884), available at https://gallica.bnf.fr/ark:/12148/bpt6k107448r/f6.image.
[66]A. C. Torres-Dias, T. F. T. Cerqueira, W. Cui, M. A. L. Marques, S. Botti, D. Machon, M. A. Hartmann, Y. Sun, D. J. Dunstan, and A. San-Miguel, Carbon **123**, 145 (2017).
[67]R. S. Alencar, W. Cui, A. C. Torres-Dias, T. F. T. Cerqueira, S. Botti, M. A. L. Marques, O. P. Ferreira, C. Laurent, A. Weibel, D. Machon, D. J. Dunstan, A. G. Souza Filho, and A. San-Miguel, Carbon **125**, 429 (2017).
[68]F. Balima, S. Le Floch, C. Adessi, T. F. T. Cerqueira, N. Blanchard, R. Arenal, A. Brûlet, M. A. L. Marques, S. Botti, and A. San-Miguel, Carbon **106**, 64 (2016).
[69]J. Zang, A. Treibergs, Y. Han, and F. Liu, Phys. Rev. Lett. **92**, 105501 (2004).
[70]P. Puech, E. Flahaut, A. Sapelkin, H. Hubel, D. J. Dunstan, G. Landa, and W. S. Bacsa, Phys. Rev. B **73**, 233408 (2006).
[71]S. You, M. Masses, I. Dobryden, A. A. Green, M. C. Hersam, and A. V. Soldatov, High Press. Res. **31**, 186 (2011).
[72]R. S. Alencar, A. L. Aguiar, A. R. Paschoal, P. T. C. Freire, Y. A. Kim, H. Muramatsu, M. Endo, H. Terrones, M. Terrones, A. San-Miguel, M. S. Dresselhaus, and A. G. Souza Filho, J. Phys. Chem. C **118**, 8153 (2014).
[73]V. Perebeinos and J. Tersoff, Nano Lett. **14**, 4376 (2014).
[74]C. E. Giusca, Y. Tison, and S. R. P. Silva, Phys. Rev. B **76**, 035429 (2007).
[75]S. Reich, C. Thomsen, and P. Ordejón, Phys. Rev. B **65**, 153407 (2002).
[76]R. B. Capaz, C. D. Spataru, P. Tangney, M. L. Cohen, and S. G. Louie, Phys. Status Solidi B-Basic Solid State Phys. **241**, 3352 (2004).
[77]R. S. Deacon, K.-C. Chuang, J. Doig, I. B. Mortimer, and R. J. Nicholas, Phys. Rev. B **74**, 201402 (2006).
[78]A. C. Torres-Dias, S. Cambré, W. Wenseleers, D. Machon, and A. San-Miguel, Carbon **95**, 442 (2015).
[79]L. Saviot, A. Mermet, and E. Duval, *Handbook of Nanophysics: Nanoparticles and Quantum Dots*, edited by K. D. Sattler (CRC Press, 2010), pp. 11.1–11.16.

[80]H. T. Girão, T. Cornier, S. Daniele, R. Debord, M. A. Caravaca, R. A. Casali, P. Mélinon, and D. Machon, J. Phys. Chem. C **121**, 15463 (2017).
[81]L. Saviot, D. Machon, A. Mermet, D. B. Murray, S. Adichtchev, J. Margueritat, F. Demoisson, M. Ariane, M. del C, and M. de Lucas, J. Phys. Chem. C **116**, 22043 (2012).
[82]A. Girard, J. Ramade, J. Margueritat, D. Machon, L. Saviot, F. Demoisson, and A. Mermet, Nanoscale **10**, 2154 (2018).
[83]R. Ruoff, J. Tersoff, D. Lorents, S. Subramoney, and B. Chan, Nature **364**, 514 (1993).
[84]T. Hertel, R. E. Walkup, and P. Avouris, Phys. Rev. B **58**, 13870 (1998).
[85]J.-C. Blancon, M. Paillet, H. N. Tran, X. T. Than, S. A. Guebrou, A. Ayari, A. San Miguel, N.-M. Phan, A.-A. Zahab, J.-L. Sauvajol, N. Del Fatti, and F. Vallee, Nat. Commun. **4**, 2542 (2013).
[86]Y. W. Sun, I. Hernández, J. González, K. Scott, K. J. Donovan, A. Sapelkin, F. Rodríguez, and D. J. Dunstan, J. Phys. Chem. C **120**, 1863 (2016).
[87]A. Merlen, P. Toulemonde, N. Bendiab, A. Aouizerat, J. L. Sauvajol, G. Montagnac, H. Cardon, P. Petit, and A. S. Miguel, Phys. Status Solidi B **243**, 690 (2006).
[88]A. J. Ghandour, I. F. Crowe, J. E. Proctor, Y. W. Sun, M. P. Halsall, I. Hernandez, A. Sapelkin, and D. J. Dunstan, Phys. Rev. B **87**, 085416 (2013).
[89]W. Cui, T. F. T. Cerqueira, S. Botti, M. A. L. Marques, and A. San-Miguel, Phys. Chem. Chem. Phys. **18**, 19926 (2016).
[90]A. Merlen, P. Toulemonde, S. Le Floch, G. Montagnac, T. Hammouda, O. Marty, and A. San Miguel, Carbon **47**, 1643 (2009).
[91]M. Noël, S. Ananev, M. Mases, X. Devaux, J. Lee, I. Evdokimov, M. Dossot, E. McRae, and A. V. Soldatov, Phys. Status Solidi Rapid Res. Lett. **8**, 935 (2014).
[92]L. A. Chernozatonskii, Chem. Phys. Lett. **297**, 257 (1998).
[93]Y.-N. Xu, M.-Z. Huang, and W. Y. Ching, Phys. Rev. B **46**, 4241 (1992).
[94]B. Sundqvist, Adv. Phys. **48**, 1 (1999).
[95]B. Sundqvist, in *Fuller.-Based Mater.*, edited by K. Prassides (Springer, Berlin, 2004), pp. 85–126.
[96]V. D. Blank, S. G. Buga, G. A. Dubitsky, N. R. Serebryanaya, M. Y. Popov, and B. Sundqvist, Carbon **36**, 319 (1998).
[97]V. D. Blank, S. G. Buga, N. R. Serebryanaya, V. N. Denisov, G. A. Dubitsky, A. N. Ivlev, B. N. Mavrin, and M. Y. Popov, Phys. Lett. A **205**, 208 (1995).
[98]E. Burgos, E. Halac, R. Weht, H. Bonadeo, E. Artacho, and P. Ordejón, Phys. Rev. Lett. **85**, 2328 (2000).
[99]S. Yamanaka, A. Kubo, K. Inumaru, K. Komaguchi, N. S. Kini, T. Inoue, and T. Irifune, Phys. Rev. Lett. **96**, 076602 (2006).
[100]L. Chernozatonskii, N. Serebryanaya, and B. Mavrin, Chem. Phys. Lett. **316**, 199 (2000).
[101]M. Popov, V. Mordkovich, S. Perfilov, A. Kirichenko, B. Kulnitskiy, I. Perezhogin, and V. Blank, Carbon **76**, 250 (2014).
[102]K. P. Meletov, G. A. Kourouklis, J. Arvanitidis, K. Prassides, and Y. Iwasa, Phys. Rev. B **68**, 094103 (2003).
[103]J. Léger, J. Haines, V. Davydov, and V. Agafonov, Solid State Commun. **121**, 241 (2002).
[104]F. Moshary, N. H. Chen, I. F. Silvera, C. A. Brown, H. C. Dorn, M. S. de Vries, and D. S. Bethune, Phys. Rev. Lett. **69**, 466 (1992).
[105]B. Sundqvist, Carbon **125**, 258 (2017).
[106]L. Marques, Y. Skorokhod, and R. Soares, Carbon **82**, 599 (2015).
[107]L. Marques, Y. Skorokhod, and R. Soares, Phys. Status Solidi-Rapid Res. Lett. **9**, 535 (2015).
[108]J. Proctor, E. Gregoryanz, K. Novoselov, M. Lotya, J. Coleman, and M. Halsall, Phys. Rev. B **80**, 073408 (2009).
[109]K. Filintoglou, N. Papadopoulos, J. Arvanitidis, D. Christofilos, O. Frank, M. Kalbac, J. Parthenios, G. Kalosakas, C. Galiotis, and K. Papagelis, Phys. Rev. B **88**, 045418 (2013).
[110]A. P. Nayak, T. Pandey, D. Voiry, J. Liu, S. T. Moran, A. Sharma, C. Tan, C.-H. Chen, L.-J. Li, M. Chhowalla, J.-F. Lin, A. K. Singh, and D. Akinwande, Nano Lett. **15**, 346 (2015).
[111]R. S. Alencar, K. D. A. Saboia, D. Machon, G. Montagnac, V. Meunier, O. P. Ferreira, A. San-Miguel, and A. G. Souza Filho, Phys. Rev. Mater. **1**, 024002 (2017).
[112]C. Bousige, F. Balima, D. Machon, G. S. Pinheiro, A. Torres-Dias, J. Nicolle, D. Kalita, N. Bendiab, L. Marty, V. Bouchiat, G. Montagnac, A. G. Souza Filho, P. Poncharal, and A. San-Miguel, Nano Lett. **17**, 21 (2017).
[113]N. S. Mueller, S. Heeg, M. P. Alvarez, P. Kusch, S. Wasserroth, N. Clark, F. Schedin, J. Parthenios, K. Papagelis, C. Galiotis, M. Kalbáč, A. Vijayaraghavan, U. Huebner, R. Gorbachev, O. Frank, and S. Reich, 2D Mater. **5**, 015016 (2018).
[114]M. Riccò, M. Belli, D. Pontiroli, M. Mazzani, T. Shiroka, D. Arčon, A. Zorko, S. Margadonna, and G. Ruani, Phys. Rev. B **75**, 081401 (2007).
[115]K. Tanigaki, T. W. Ebbesen, S. Saito, J. Mizuki, J. S. Tsai, Y. Kubo, and S. Kuroshima, Nature **352**, 222 (1991).
[116]T. T. M. Palstra, O. Zhou, Y. Iwasa, P. E. Sulewski, R. M. Fleming, and B. R. Zegarski, Solid State Commun. **93**, 327 (1995).
[117]N. Rey, A. Muñoz, P. Rodríguez-Hernández, and A. San Miguel, J. Phys. Condens. Matter **20**, 215218 (2008).
[118]R. Poloni, D. Machon, M. V. Fernandez-Serra, S. Le Floch, S. Pascarelli, G. Montagnac, H. Cardon, and A. San-Miguel, Phys. Rev. B **77**, 125413 (2008).
[119]R. Poloni, G. Aquilanti, P. Toulemonde, S. Pascarelli, S. Le Floch, D. Machon, D. Martinez-Blanco, G. Morard, and A. San-Miguel, Phys. Rev. B **77**, 205433 (2008).
[120]V. Pischedda, M. Yao, R. Debord, G. Gabarino, and A. San-Miguel, J. Phys. Condens. Matter **26**, 365302 (2014).
[121]M. Yao, V. Pischedda, B. Sundqvist, T. Wågberg, M. Mezouar, R. Debord, and A. San Miguel, Phys. Rev. B **84**, 144106 (2011).
[122]V. A. Nalimova, Mol. Cryst. Liq. Cryst. Sci. Technol. Sect. Mol. Cryst. Liq. Cryst. **310**, 5 (1998).
[123]K. Mizoguchi, M. Machino, H. Sakamoto, T. Kawamoto, M. Tokumoto, A. Omerzu, and D. Mihailovic, Phys. Rev. B **63**, 140417 (2001).
[124]K. Thirunavukkuarasu, C. A. Kuntscher, B. J. Nagy, I. Jalsovszky, G. Klupp, K. Kamarás, É Kováts, and S. Pekker, J. Phys. Chem. C **112**, 17525 (2008).
[125]K. P. Meletov and D. V. Konarev, Chem. Phys. Lett. **553**, 21 (2012).
[126]L. Wang, J. Phys. Chem. Solids **84**, 85 (2015).
[127]L. Wang, B. Liu, H. Li, W. Yang, Y. Ding, S. V. Sinogeikin, Y. Meng, Z. Liu, X. C. Zeng, and W. L. Mao, Science **337**, 825 (2012).
[128]M. Yao, W. Cui, J. Xiao, S. Chen, J. Cui, R. Liu, T. Cui, B. Zou, B. Liu, and B. Sundqvist, Appl. Phys. Lett. **103**, 071913 (2013).
[129]C. Pei, M. Feng, Z. Yang, M. Yao, Y. Yuan, X. Li, B. Hu, M. Shen, B. Chen, B. Sundqvist, and L. Wang, Carbon **124**, 499 (2017).
[130]M. Du, M. Yao, J. Dong, P. Ge, Q. Dong, É Kováts, S. Pekker, S. Chen, R. Liu, B. Liu, T. Cui, B. Sundqvist, and B. Liu, Adv. Mater. **30**, 1706916 (2018).
[131]A. A. Popov, S. Yang, and L. Dunsch, Chem. Rev. **113**, 5989 (2013).
[132]M. Saunders, H. A. Jimenez-Vazquez, R. J. Cross, S. Mroczkowski, M. L. Gross, D. E. Giblin, and R. J. Poreda, J. Am. Chem. Soc. **116**, 2193 (1994).
[133]T. Oku, Energies **8**, 319 (2015).
[134]A. Iwasiewicz-Wabnig, K. Porfyrakis, G. A. D. Briggs, and B. Sundqvist, Phys. Status Solidi. B **246**, 2767 (2009).
[135]A. San-Miguel and P. Toulemonde, High Press. Res. **25**, 159 (2005).
[136]P. Toulemonde, A. San Miguel, A. Merlen, R. Viennois, S. Le Floch, C. Adessi, X. Blase, and J. Tholence, J. Phys. Chem. Solids **67**, 1117 (2006).
[137]L. Yang, C. A. Tulk, D. D. Klug, I. L. Moudrakovski, C. I. Ratcliffe, J. A. Ripmeester, B. C. Chakoumakos, L. Ehm, C. D. Martin, and J. B. Parise, Proc. Natl. Acad. Sci. **106**, 6060 (2009).
[138]K. Momma, J. Phys. Condens. Matter **26**, 103203 (2014).
[139]H. P. Veluswamy, R. Kumar, and P. Linga, Appl. Energy **122**, 112 (2014).
[140]F. Morales, M. Núñez-Regueiro, P. Toulemonde, D. Machon, S. Le Floch, V. Pischedda, P. Lagarde, A.-M. Flank, J. P. Itié, and A. San-Miguel, Phys. Rev. B **94**, 104507 (2016).
[141]H. Wang, J. S. Tse, K. Tanaka, T. Iitaka, and Y. Ma, Proc. Natl. Acad. Sci. **109**, 6463 (2012).
[142]Y. Li, J. Hao, H. Liu, J. S. Tse, Y. Wang, and Y. Ma, Sci. Rep. **5**, 9948 (2015).
[143]D. Connétable, Phys. Rev. Lett. **91**, 247001 (2003).
[144]T. Zeng, R. Hoffmann, R. Nesper, N. W. Ashcroft, T. A. Strobel, and D. M. Proserpio, J. Am. Chem. Soc. **137**, 12639 (2015).
[145]J.-A. Dolyniuk, B. Owens-Baird, J. Wang, J. V. Zaikina, and K. Kovnir, Mater. Sci. Eng. R Rep. **108**, 1 (2016).
[146]S. Yamanaka, E. Enishi, H. Fukuoka, and M. Yasukawa, Inorg. Chem. **39**, 56 (2000).
[147]S. Yamanaka, Dalton Trans. **39**, 1901 (2010).
[148]R. Viennois, P. Toulemonde, C. Paulsen, and A. San-Miguel, J. Phys. Condens. Matter **17**, L311 (2005).
[149]P. Toulemonde, C. Adessi, X. Blase, A. San Miguel, and J. Tholence, Phys. Rev. B **71**, 094504 (2005).

[150]N. Jaussaud, P. Toulemonde, M. Pouchard, A. San Miguel, P. Gravereau, S. Pechev, G. Goglio, and C. Cros, Solid State Sci. **6**, 401 (2004).
[151]E. Reny, S. Yamanaka, C. Cros, and M. Pouchard, Chem. Commun. **0**, 2505 (2000).
[152]S. Pailhès, H. Euchner, V. M. Giordano, R. Debord, A. Assy, S. Gomès, A. Bosak, D. Machon, S. Paschen, and M. de Boissieu, Phys. Rev. Lett. **113**, 025506 (2014).
[153]A. San-Miguel, P. Keghelian, X. Blase, P. Melinon, A. Perez, J. Itie, A. Polian, E. Reny, C. Cros, and M. Pouchard, Phys. Rev. Lett. **83**, 5290 (1999).
[154]A. San Miguel, A. Merlen, P. Toulemonde, T. Kume, S. Le Floch, A. Aouizerat, S. Pascarelli, G. Aquilanti, O. Mathon, T. Le Bihan, J. Itie, and S. Yamanaka, Europhys. Lett. **69**, 556 (2005).
[155]D. Machon, P. Toulemonde, P. McMillan, M. Amboage, A. Munoz, P. Rodriguez-Hernandez, and A. San Miguel, Phys. Rev. B **79**, 184101 (2009).
[156]D. Machon, P. F. McMillan, A. San-Miguel, P. Barnes, and P. T. Hutchins, *Physics and Chemistry of Inorganic Clathrates* (Springer, 2014), pp. 91–123.
[157]D. E. Sklovsky, H. Gaucher, G. N. Bondarenko, S. Menu, F. Beguin, S. Bonnamy, J. Conard, and V. A. Nalimova, Mol. Cryst. Liq. Cryst. Sci. Technol. Sect. Mol. Cryst. Liq. Cryst. **310**, 165 (1998).
[158]L. Alvarez, J.-L. Bantignies, R. Le Parc, R. Aznar, J.-L. Sauvajol, A. Merlen, D. Machon, and A. San Miguel, Phys. Rev. B **82**, 205403 (2010).
[159]W. Q. Neves, R. S. Alencar, R. S. Ferreira, A. C. Torres-Dias, N. F. Andrade, A. San-Miguel, Y. A. Kim, M. Endo, D. W. Kim, H. Muramatsu, A. L. Aguiar, and A. G. Souza Filho, Carbon **133**, 446 (2018).
[160]A. San Miguel, *High Pressure Processes in Chemical Engineering*, edited by M. Lackner (Processing Engineering GmbH, 2010) p. 413.
[161]A. Merlen, N. Bendiab, P. Toulemonde, A. Aouizerat, A. San Miguel, J. Sauvajol, G. Montagnac, H. Cardon, and P. Petit, Phys. Rev. B **72**, 035409 (2005).
[162]T. Pichler, H. Kuzmany, H. Kataura, and Y. Achiba, Phys. Rev. Lett. **87**, 267401 (2001).
[163]A. Trave, F. J. Ribeiro, S. G. Louie, and M. L. Cohen, Phys. Rev. B **70**, 205418 (2004).
[164]S. Kwasaki, Y. Matsuoka, T. Yokomae, Y. Nojima, F. Okino, H. Touhara, and H. Kataura, Carbon **43**, 37 (2005).
[165]M. Chorro, S. Rols, J. Cambedouzou, L. Alvarez, R. Almairac, J.-L. Sauvajol, J.-L. Hodeau, L. Marques, M. Mezouar, and H. Kataura, Phys. Rev. B **74**, 205425 (2006).
[166]M. Chorro, J. Cambedouzou, A. Iwasiewicz-Wabnig, L. Noé, S. Rols, M. Monthioux, B. Sundqvist, and P. Launois, Europhys. Lett. **79**, 56003 (2007).
[167]A. L. Aguiar, E. B. Barros, V. P. Sousa Filho, H. Terrones, V. Meunier, D. Machon, Y. A. Kim, H. Muramatsu, M. Endo, F. Baudelet, A. San-Miguel, and A. G. Souza Filho, J. Phys. Chem. C **121**, 10609 (2017).
[168]Z. Yao, J. Zhang, M.-G. Yao, S.-L. Chen, and B.-B. Liu, J. Phys. Chem. C **120**, 23189 (2016).
[169]X. Yang, M. Yao, J. Zhang, Z. Yao, S. Chen, M. Du, H. Li, P. Shen, R. Liu, T. Cui, B. Sundqvist, and B. Liu, J. Raman Spectrosc. **48**, 951 (2017).
[170]Y. Tian, B. Xu, D. Yu, Y. Ma, Y. Wang, Y. Jiang, W. Hu, C. Tang, Y. Gao, K. Luo, Z. Zhao, L.-M. Wang, B. Wen, J. He, and Z. Liu, Nature **493**, 385 (2013).
[171]N. Ishimatsu, K. Matsumoto, H. Maruyama, N. Kawamura, M. Mizumaki, H. Sumiya, and T. Irifune, J. Synchrotron Radiat. **19**, 768 (2012).
[172]A. V. Ragulya, Adv. Appl. Ceram. **107**, 118 (2008).
[173]R. Chaim, M. Levin, A. Shlayer, and C. Estournes, Adv. Appl. Ceram. **107**, 159 (2008).
[174]J. A. Wollmershauser, B. N. Feigelson, E. P. Gorzkowski, C. T. Ellis, R. Goswami, S. B. Qadri, J. G. Tischler, F. J. Kub, and R. K. Everett, Acta Mater. **69**, 9 (2014).
[175]B. Jiang, Int. J. Plast. **20**, 2007 (2004).
[176]I. Issa, L. Joly-Pottuz, J. Réthoré, C. Esnouf, T. Douillard, V. Garnier, J. Chevalier, S. Le Floch, D. Machon, and K. Masenelli-Varlot, Acta Mater. **150**, 308 (2018).
[177]V. L. Solozhenko, O. O. Kurakevych, and Y. Le Godec, Adv. Mater. **24**, 1540 (2012).
[178]N. Nishiyama, S. Seike, T. Hamaguchi, T. Irifune, M. Matsushita, M. Takahashi, H. Ohfuji, and Y. Kono, Scr. Mater. **67**, 955 (2012).
[179]F. Maglia, I. G. Tredici, and U. Anselmi-Tamburini, J. Eur. Ceram. Soc. **33**, 1045 (2013).
[180]D.-L. Yung, S. Cygan, M. Antonov, L. Jaworska, and I. Hussainova, Int. J. Refract. Met. Hard Mater. **61**, 201 (2016).
[181]F. Balima, F. Bellin, D. Michau, O. Viraphong, A. Poulon-Quintin, U.-C. Chung, A. Dourfaye, and A. Largeteau, Mater. Des. **139**, 541 (2018).
[182]Y. Le Godec, S. Le Floch, S. Pailhès, and J.-M. Combes, Patent WO2018083325 (A1) (11 May 2018).
[183]T. Yildirim, O. Gülseren, Ç Kılıç, and S. Ciraci, Phys. Rev. B **62**, 12648 (2000).
[184]M. Sakurai and S. Saito, Physica E **43**, 673 (2011).
[185]L. G. P. Martins, M. J. S. Matos, A. R. Paschoal, P. T. C. Freire, N. F. Andrade, A. L. Aguiar, J. Kong, B. R. A. Neves, A. B. de Oliveira, M. S. C. Mazzoni, A. G. S. Filho, and L. G. Cançado, Nat. Commun. **8**, 96 (2017).
[186]S. S. Coutinho, V. Lemos, and S. Guerini, Phys. Rev. B **80**, 193408 (2009).
[187]L. B. da Silva, S. B. Fagan, and R. Mota, Nano Lett. **4**, 65 (2004).
[188]C. Caillier, A. Ayari, V. Gouttenoire, A. San Miguel, V. Jourdain, M. Picher, and J. Sauvajol, Appl. Phys. Lett. **97**, 173111 (2010).
[189]C. F. Burmeister and A. Kwade, Chem. Soc. Rev. **42**, 7660 (2013).
[190]Y. Estrin and A. Vinogradov, Acta Mater. **61**, 782 (2013).
[191]A. W. Weeber and H. Bakker, Phys. B Condens. Matter **153**, 93 (1988).
[192]S. D. Silva-Santos, R. S. Alencar, A. L. Aguiar, Y. A. Kim, H. Muramatsu, M. Endo, N. P. Blanchard, A. San-Miguel, and A. G. Souza Filho, Carbon **141**, 568 (2019).
[193]X. Yang, M. Yao, X. Wu, S. Liu, S. Chen, K. Yang, R. Liu, T. Cui, B. Sundqvist, and B. Liu, Phys. Rev. Lett. **118**, 245701 (2017).
[194]M. S. Dresselhaus, G. Dresselhaus, A. Jorio, A. G. Souza Filho, and R. Saito, Carbon **40**, 2043 (2002).
[195]D. Christofilos, J.-C. Blancon, J. Arvanitidis, A. San Miguel, A. Ayari, N. Del Fatti, and F. Vallee, J. Phys. Chem. Lett. **3**, 1176 (2012).
[196]M.-I. Richard, S. Fernández, J. Eymery, J. P. Hofmann, L. Gao, J. Carnis, S. Labat, V. Favre-Nicolin, E. J. M. Hensen, O. Thomas, T. U. Schülli, and S. J. Leake, Nanoscale **10**, 4833 (2018).